AD-773 660

ADVANCED ENGINE CONTROL PROGRAM

R. J. Hearn, et al

Colt Industries, Incorporated

Prepared for:

Army Air Mobility Research and Development Laboratory

November 1973

DISCLAIMERS

The findings in this report are not to be construed as an official Department of the Army position unless so designated by other authorized documents.

When Government drawings, specifications, or other data are used for any purpose other than in connection with a definitely related Government procurement operation, the United States Government thereby incurs no responsibility nor any obligation whatsoever; and the fact that the Government may have formulated, furnished, or in any way supplied the said drawings, specifications, or other data is not to be regarded by implication or otherwise as in any manner licensing the holder or any other person or corporation, or conveying any rights or permission, to manufacture, use, or sell any patented invention that may in any way be related thereto.

Trade names cited in this report do not constitute an official endorsement or approval of the use of such commercial hardware or software.

DISPOSITION INSTRUCTIONS

Destroy this report when no longer needed. Do not return it to the originator.

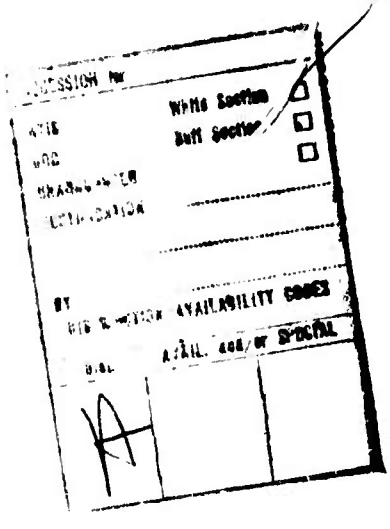

Unclassified

Security Classification

AD773-660

DOCUMENT CONTROL DATA - R & D

(Security classification of title, body of abstract and indexing annotation must be entered when the overall report is classified)

1. ORIGINATING ACTIVITY (Corporate author) Colt Industries, Inc. Chandler Evans Control Systems Division West Hartford, Connecticut	2a. REPORT SECURITY CLASSIFICATION Unclassified 2b. GROUP

3. REPORT TITLE

ADVANCED ENGINE CONTROL PROGRAM

4. DESCRIPTIVE NOTES (Type of report and inclusive dates)

Final Report

5. AUTHOR(S) (First name, middle initial, last name)

R. J. Hearn
M. A. Cole
A. H. White

6. REPORT DATE	7a. TOTAL NO. OF PAGES	7b. NO. OF REFS
November 1973	94	16

8a. CONTRACT OR GRANT NO.	9a. ORIGINATOR'S REPORT NUMBER(S)
DAAJ02-72-C-0084 b. PROJECT NO. Task 1G162207AA7103 c. d.	USAAMRDL Technical Report 72-59 9b. OTHER REPORT NO(S) (Any other numbers that may be assigned this report) Chandler Evans Report R-492-45

10. DISTRIBUTION STATEMENT

Approved for public release; distribution unlimited.

11. SUPPLEMENTARY NOTES	12. SPONSORING MILITARY ACTIVITY
	Eustis Directorate, U. S. Army Air Mobility R & D Laboratory Fort Eustis, Virginia

13. ABSTRACT

This report describes the results of a 12-month program to continue development of electronic control and centrifugal pump technology for use in future small (2- to 5-lb-per-second airflow) turboshaft engines. Previous development work under Contract DAAJ02-70-C-0002 defined technical deficiencies in these areas.

Redesign of the electronic computer using micropowered analog and digital components has resulted in a reduction in electrical power dissipation from 60 to about 7 watts, which virtually eliminates self-heating problems. Supply voltage and noise sensitivities have also been substantially reduced. The induced vibration has been limited to less than 30 g's over the complete vibration spectrum specified in MIL-E-5007C. This was accomplished by using a combination of PCB viscoelastic damping material and vibration isolation.

Increasing the pump speed from 37,500 to 55,000 rpm to reduce disc friction has resulted in a 50% reduction in the fuel temperature rise. Further improvements in pump efficiency were demonstrated by operating the pump in the vapor core mode (throttled inlet).

DD FORM 1 NOV 68 1473 REPLACES DD FORM 1473, 1 JAN 64, WHICH IS OBSOLETE FOR ARMY USE.

Unclassified

Security Classification

14. KEY WORDS	LINK A		LINK B		LINK C	
	ROLE	WT	ROLE	WT	ROLE	WT
Electronic Engine Mounted Control Turboshaft Engine Fuel Cooled Electronic Computer Fuel Pump Alternator						

DEPARTMENT OF THE ARMY
U. S. ARMY AIR MOBILITY RESEARCH & DEVELOPMENT LABORATORY
EUSTIS DIRECTORATE
FORT EUSTIS, VIRGINIA 23604

The research described herein was conducted by Chandler Evans Control Systems Division of Colt Industries under Contract DAAJ02-72-C-0084. The work was performed under the technical management of Mr. R.G. Furgurson, Propulsion Technical Area, Technology Applications Division, Eustis Directorate.

The objective of this program was to improve several technical design deficiencies in the electronic system and fuel pumping system of the engine controls investigated previously under U.S. Army Contract DAAJ02-70-C-0002. A redesign of the electronic control package resulted in a much more compact and rugged unit almost totally free from objectionable internal heating. The centrifugal fuel pump previously investigated was redesigned to reduce the problem of engine fuel heating. The improvement objectives in both the electronic system and the centrifugal fuel pump were validated by component testing.

Appropriate technical personnel of this Directorate have reviewed this report and concur with the conclusions contained herein.

ic

Task 1G162207AA7103
Contract DAAJ02-72-C-0084
USAAMRDL Technical Report 73-81
November 1973

ADVANCED ENGINE CONTROL PROGRAM

Final Report

Chandler Evans Report R-492-45

By

R. J. Hearn
M. A. Cole
A. H. White

Prepared by

Colt Industries
Chandler Evans Control Systems Division
West Hartford, Connecticut

for

EUSTIS DIRECTORATE
U. S. ARMY AIR MOBILITY RESEARCH AND DEVELOPMENT LABORATORY
FORT EUSTIS, VIRGINIA

ABSTRACT

This report describes the results of a 12-month program to continue development of electronic control and centrifugal pump technology for use in future small (2- to 5-lb-per-second airflow) turboshaft engines. Previous development work under Contract DAAJ02-70-C-0002 defined technical deficiencies in these areas.

Redesign of the electronic computer using micropowered analog and digital components has resulted in a reduction in electrical power dissipation from 60 to about 7 watts, which virtually eliminates self-heating problems. Supply voltage and noise sensitivities have also been substantially reduced. The induced vibration has been limited to less than 30 g's over the complete vibration spectrum specified in MIL-E-5007C. This was accomplished by using a combination of PCB viscoelastic damping material and vibration isolation.

Increasing the pump speed from 37,500 to 55,000 rpm to reduce disc friction has resulted in a 50% reduction in the fuel temperature rise. Further improvements in pump efficiency were demonstrated by operating the pump in the vapor core mode (throttled inlet).

FOREWORD

This is the final report covering work completed under Contract DAAJ02-72-C-0084 (DA Task 1G162207AA7103). The program was conducted under the direction of Mr. Roger Furgurson, Eustis Directorate, U. S. Army Air Mobility Research and Development Laboratory. The program was conducted by Colt Industries, Chandler Evans Control System Division, under the cognizance of Mr. D. F. Wills, Vice President of Engineering, and Mr. J. M. Maljanian, Manager of Fuel Controls. Mr. A. H. White was the program manager, and Mr. M. A. Cole and Mr. R. J. Hearn were the principal investigators.

Acknowledgment is given to Barry, Division of Barry Wright Corporation, Watertown, Massachusetts, for their assistance in evolving the vibration isolation/damping concept developed in the program.

TABLE OF CONTENTS

LIST OF ILLUSTRATIONS

LIST OF ILLUSTRATIONS (Cont)

LIST OF TABLES

LIST OF SYMBOLS

D	diameter
3D	three dimensional
EMI	electromagnetic interference
FET	field effect transistor
g	gravitational acceleration 32.2 ft/sec^2
h	film coefficient, $Btu/hr\ ft^2{}^\circ F$
HP	horsepower
Hz	frequency, cycles per second
I.C.	integrated circuit
IGV	inlet guide vane
LSI	large-scale integrated circuits
MMV	main metering valve
MSI	medium-scale integrated circuits
N	speed, rpm
N_{ft}	free turbine speed, rpm
N_{ftr}	free turbine reference speed, rpm
N_g	gas generator speed, rpm
N_{gr}	gas generator reference speed, rpm
P	pressure, psia
PLA	power lever angle, deg

LIST OF SYMBOLS (Cont)

pph	pounds per hour
pps	pounds per second
P_{t3}	compressor discharge total pressure, psia
Q_{so}	output shaft torque other engine, ft-lb
Q_{st}	output shaft torque this engine, ft-lb
ROM	read only memory
RFI	radio frequency interference
T	temperature, °R
t	time, sec
T_{t2}	compressor inlet total temperature, °R
T_{4B}	turbine blade temperature, °R
T_{4Br}	turbine blade reference temperature, °R
V	voltage
V_g	gas velocity, ft/sec
VCO	voltage-controlled oscillator
W	watts
β	collective pitch, deg
ΔT	increment of temperature, °F, °R
η_o	efficiency (overall)
θ	temperature correction, $\frac{T_{t2}}{519°R}$

LIST OF SYMBOLS (Cont)

μ	micro (10^{-6})
τ	time constant, sec

INTRODUCTION

During the past several years, significant reductions have been made in the weight, volume, and SFC of small turboshaft engines. This has been accomplished through increases in speed, compressor pressure ratio, and cycle temperature. The penalty for these improvements is a more complex engine, which includes requirements for turbine cooling, more exotic materials, variable geometry, and more sophisticated control systems.

The higher cycle temperatures in advanced engines make it necessary to sense engine temperature to optimize engine performance and to provide overtemperature protection. To make miniaturized high-speed engine gearboxes possible, appropriate sensors and high-speed pumps must be developed. Both high-speed and high-temperature sensing are more readily done using electronic sensors, which naturally leads to electronic computation. Electronic control offers flexibility for wide application and improved controllability, which can alleviate many of the problems experienced on past and present engine control systems.

An overview of the control system previously developed under Army Contract DAAJ02-70-C-0002 is shown in Figure 1. This figure describes the engine configuration, control inputs and sensed parameters, and interconnections between the control components and the engine. Figure 2 shows a system component diagram which describes the various sensors, control components, input/output signals, and all of the interfaces. A summary of the control system specification is shown in Table I. The main features of the engine-mounted control system are outlined below.

Fluid Controller Section

Fuel Pump, Fuel Metering, Manual Shutoff

Backup Manual Fuel Control

Field Controled Alternator for Control and Ignition Power

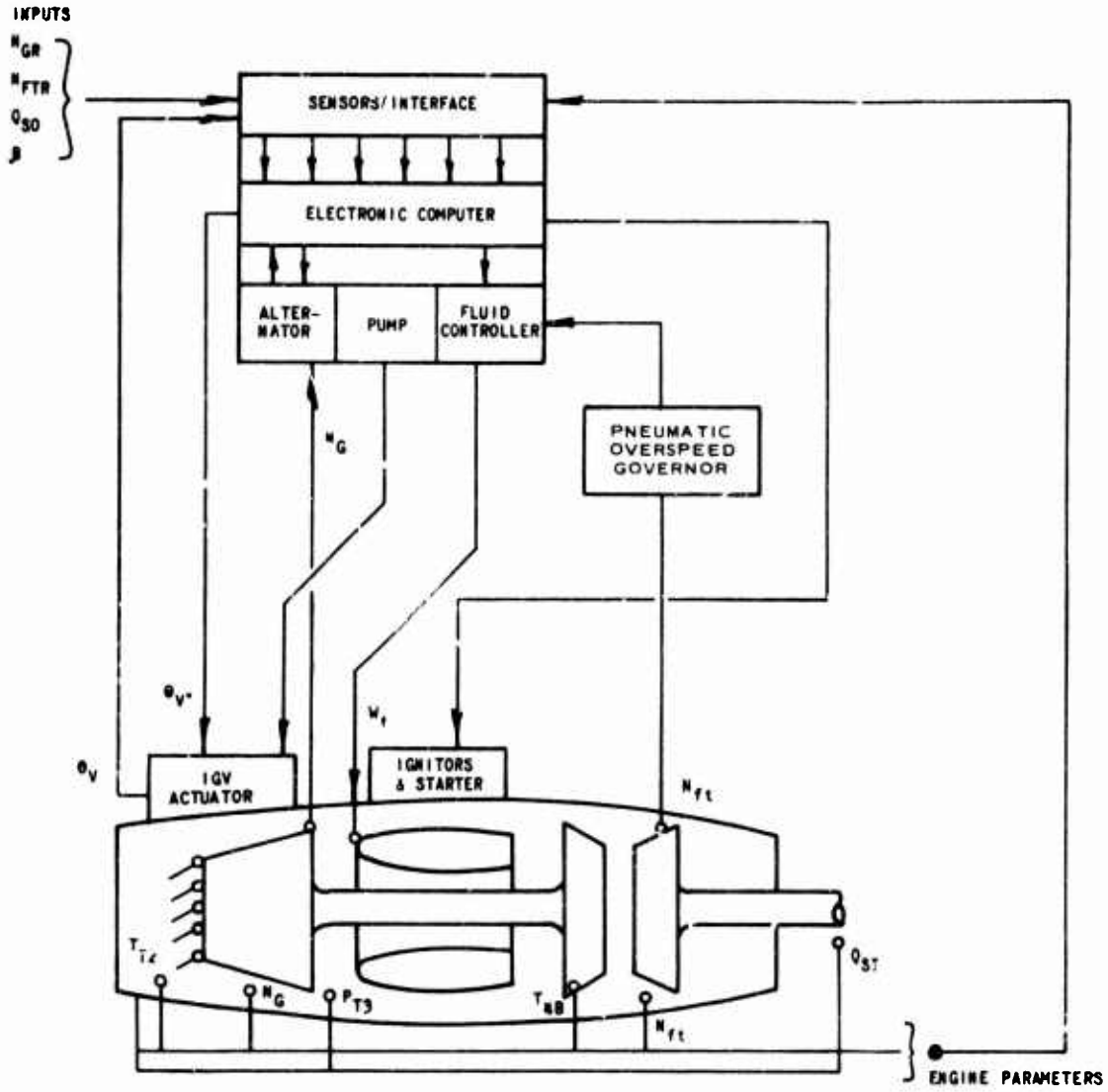

Figure 1. Engine Control System.

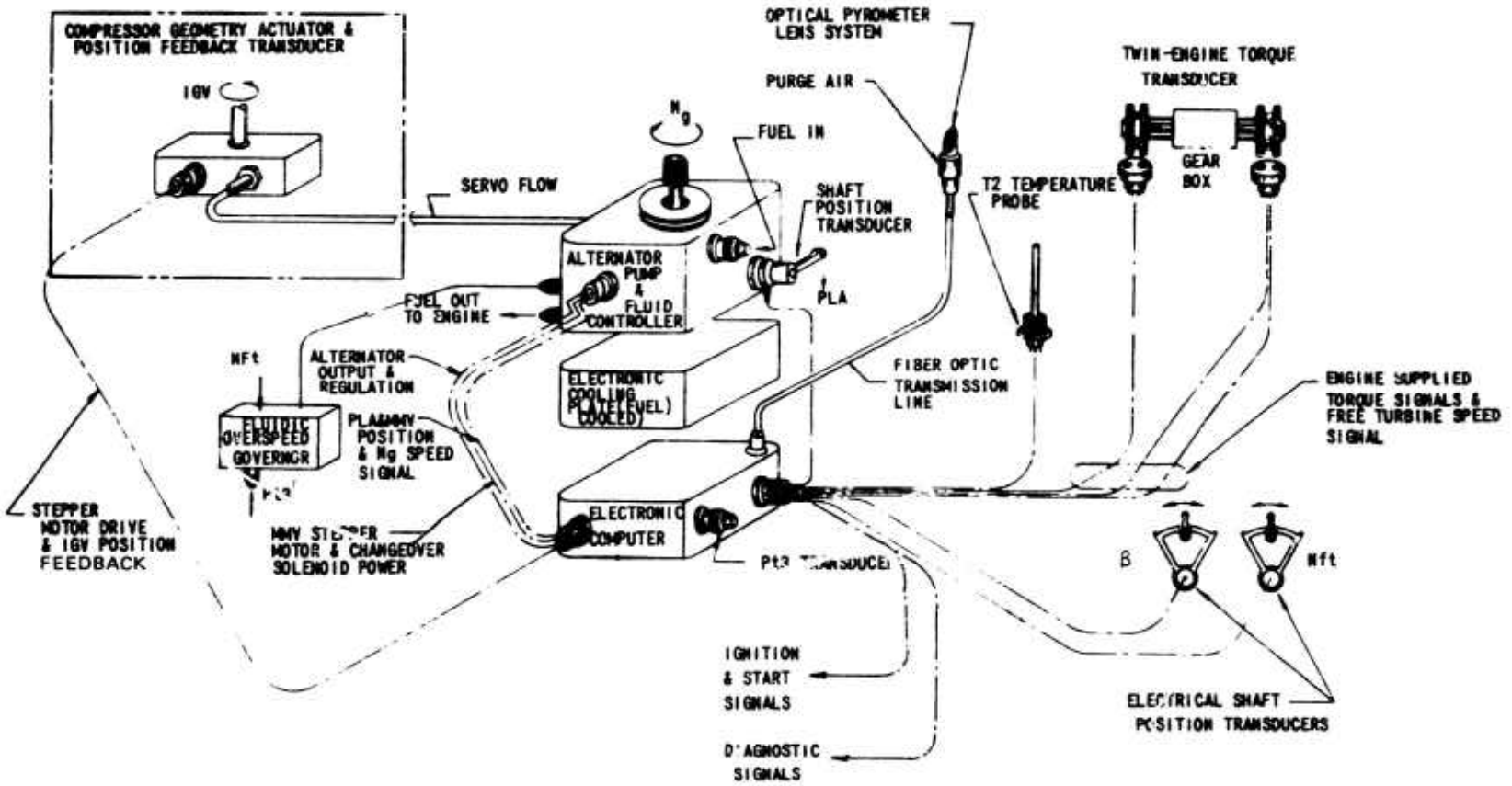

Figure 2. System Component Diagram.

TABLE I. CONTROL SPECIFICATION SUMMARY (TWIN-ENGINE HELICOPTER APPLICATION)	
Turbine Blade Temperature Limiting*	±30°F
W_F/P_{t3} Start, Acceleration & Deceleration	±2pph, ±4%, ±7.5%
Isochronous Power Turbine Governing	±.25%
Proportional Gas Producer Governing	±1%
Semiautomatic Start**	W_F = f (PLA)
Twin-Engine Load Sharing	±5% Torque
Torque Limiting*	115% ±5%
Engine Malfunction Protection (Twin Installation)	Pilot Indication
Variable Compressor Geometry Scheduling $f(N\sqrt{\theta})$	±1.5%
Load Anticipation	Collective Pitch
Proportional Power Turbine Overspeed Protection	.05 Sec Response
Manual Emergency System	Pilot Actuated
Ground & Flight Idle and Military Speed Set	Independently Adjustable
Fuel Inlet Temperature	-65° to 135°F
Ambient Temperature	-65° to 250°F
Vibration and Fuel Contamination	MIL-E-5007C

*Pilot can reset to higher limits for emergency PLA setting.

**Pilot initiates fuel flow on moving PLA to ground idle setting.

Electronic Computer Section

Hybrid Electronic Computer

Electrically Programmable 3-D Cam Using a ROM

Turbine Blade Temperature Sensor (Radiation Pyrometer)

P_{t3} Sensor (Variable Capacitance)

Cooling Plate (Fuel Cooled)

Electronics Immersed in a Heat Convective Dielectric Fluid

Geometry Actuation

Electrohydromechanical Actuator

Backup Control During Manual Fuel Control

Special Features

System Weight	15 lb
Pump/Alternator Speed	37,500 rpm
Operates on Contaminated Fuel	MIL-E-5007C
Closed-Loop Turbine Blade Temperature Limiter	

The results of the development work conducted on the control system described above defined technical deficiencies in the electronic control and centrifugal pump.

The centrifugal pump efficiency problem is caused primarily by disc friction, which is evidenced by high fuel temperature rise at off-design operating conditions. At high speed, low fuel flow and 135°F inlet fuel, the pump discharge temperature

was in the region of fuel coking (325°F). Analysis showed that by redesigning the pump for operation at 55,000 instead of 37,500 rpm, the disc diameter would be reduced, and thereby disc friction would be decreased. Also, pump performance could be improved by operating the pump in the vapor core mode.

The electronic computer had to be immersed in a dielectric fluid to provide an efficient heat transfer medium, but at a penalty in weight and vulnerability. This was necessary to convect the electronic heat to the cold plate. Although the dielectric fluid provided a good vibration medium, vibration susceptibility was still a problem area because of the inherent high resonant characteristic of the PCB's. Sensitivity to voltage and noise also required improvement.

The development work conducted during this program was undertaken to improve the electronic computer and centrifugal pump design in the technical risk areas alluded to above.

FUEL PUMP

Fuel Pump Development

The centrifugal pump developed during the previous AMRDL contract produced the required head and pressure, but it was found to be inefficient to the extent that temperature rise at the high turndown conditions resulted in excess fuel temperatures, as shown by the upper curve of Figure 3.

Design conditions for this pump were:

Δp	850 psi
Flow	450 pph
RPM	37,500

which set the specific speed of the main stage impeller to be 114.

Calculations based on the work of Daily & Nece, Trans. ASME Series D Journal of Basic Engineering, Vol. 82, 1960, pp 217-232, indicated that the major loss of power was in the form of disc friction or the impeller. The purpose of this series of tests was to demonstrate an improvement in temperature rise by an impeller designed to operate at higher shaft speed and, therefore, higher specific speed. Also, additional performance improvement could be gained by operating the pump in the vapor core mode.

The centrifugal pumps tested in this program have been run at speeds up to 55,000 rpm. Output flows of 450 pph and discharge pressures of 790 psi were achieved. They have been operated both in the "discharge throttled" mode and "inlet throttled" mode. The latter mode is most often referred to as the "vapor core" mode.

The major problem encountered in the development of these pumps has been their overall efficiency. Low efficiency results in high fuel temperature rises across the pump and, of course, increased shaft work. Development work to date has been concentrated on this problem. The following conclusions can be made

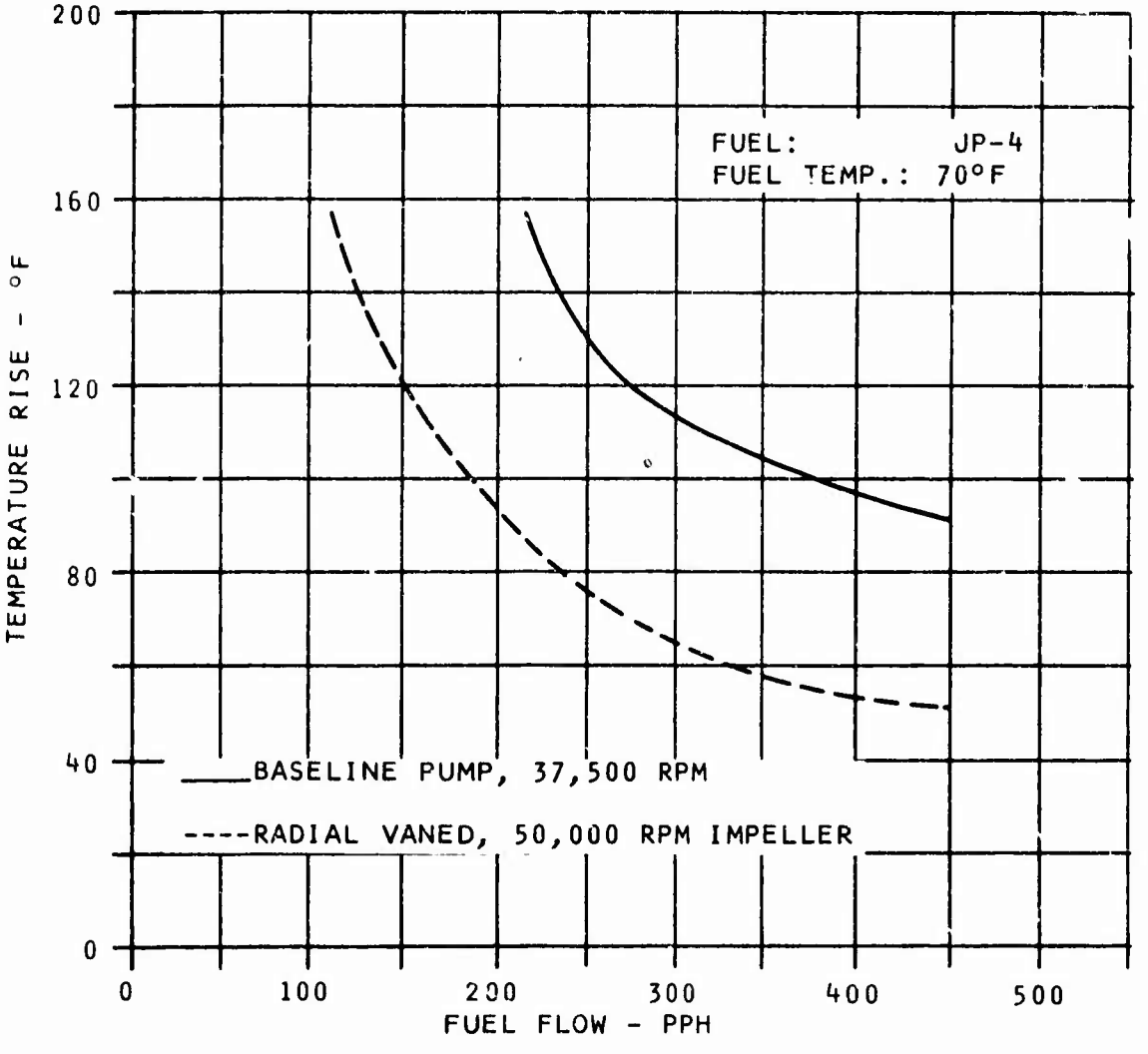

Figure 3. Temperature Rise Comparison at 100% RPM.

as a result of this work:

1. Pump performance at the higher speeds in terms of output flow and pressure does not appear to present any problems.

2. Thrust balance of the impeller is very important in these small, high-speed pumps. Proper balance results in a marked increase in overall efficiency.

3. The major cause of the low overall efficiency obtained is due to disc friction or viscous work losses.

4. Increasing pump speed for these low specific speed pumps reduces impeller diameter and in turn reduces disc friction losses. Considerable increased overall efficiency results from higher shaft speeds. This is shown by comparison in Figure 3.

5. The use of a radial vaned impeller rather than a curved vane design for a specific pump requirement results in a smaller diameter impeller. Reduced disc friction losses and increased overall efficiency result.

6. By operating the centrifugal pump in the "vapor core" mode, viscous losses and flow work are reduced. Overall pumping system efficiency is increased as demonstrated by the temperature rise reduction shown in Figures 4 and 5.

7. Operation of the pump designed for 55,000 rpm demonstrated performance of the unit within the allowable temperature rise limits for the 5-pps engine, as shown in Figure 6.

8. Analytical studies show that a 75,000-rpm impeller meets the temperature rise requirements of the 2-pps engine. See Figure 7.

9. Vapor core operation was required to use the 55,000-rpm pump for the 2-pps engine to meet the temperature rise requirements. Test results are shown in Figure 8.

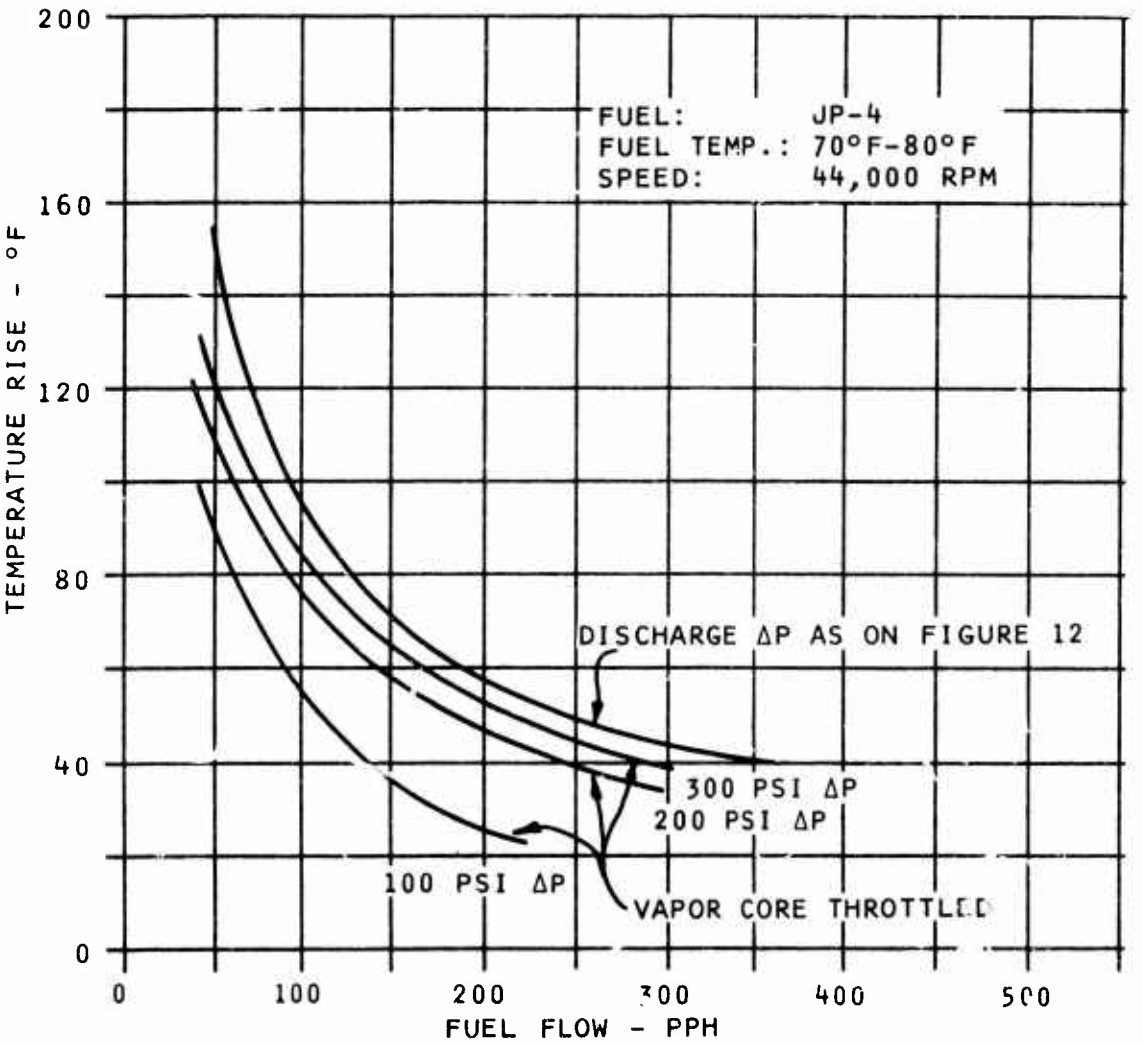

Figure 4. Temperature Rise vs. Fuel Flow for 55,000-RPM Pump at 44,000 PPM.

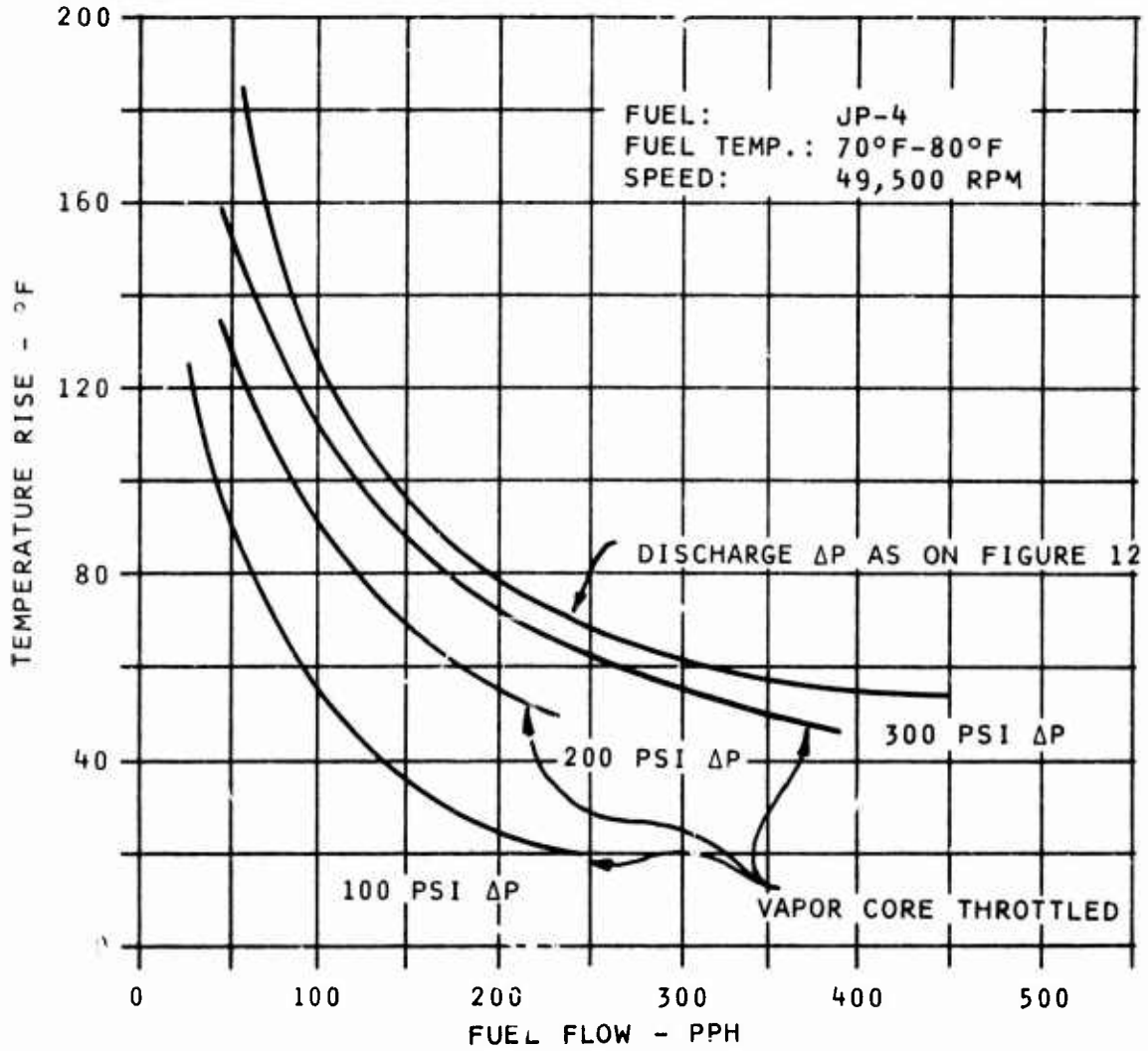

Figure 5. Temperature Rise vs. Fuel Flow for 55,000-RPM Pump at 49,500 RPM.

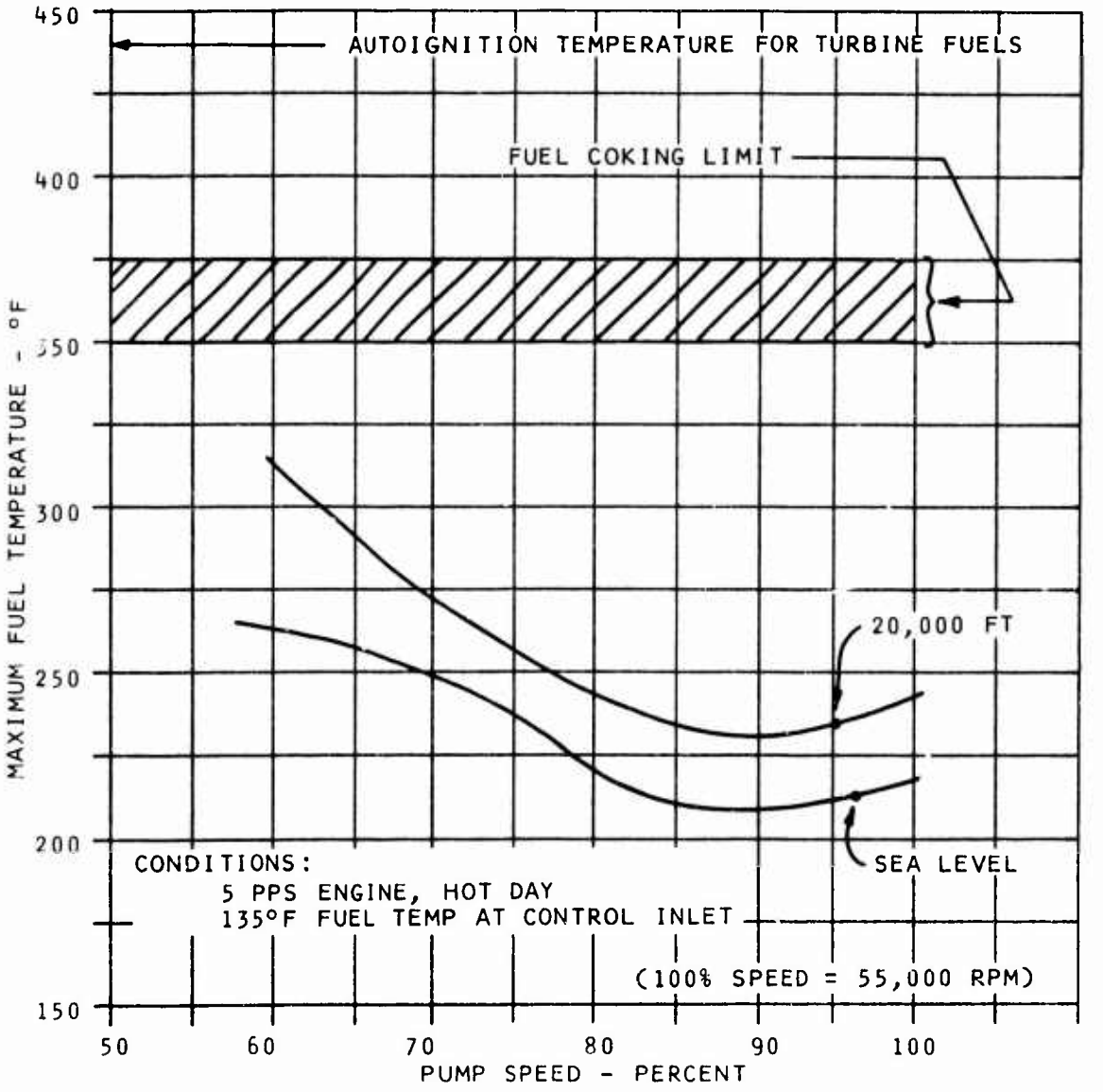

Figure 6. Maximum Steady-State Fuel Temperature, 5-PPS Engine - 55,000-RPM Pump.

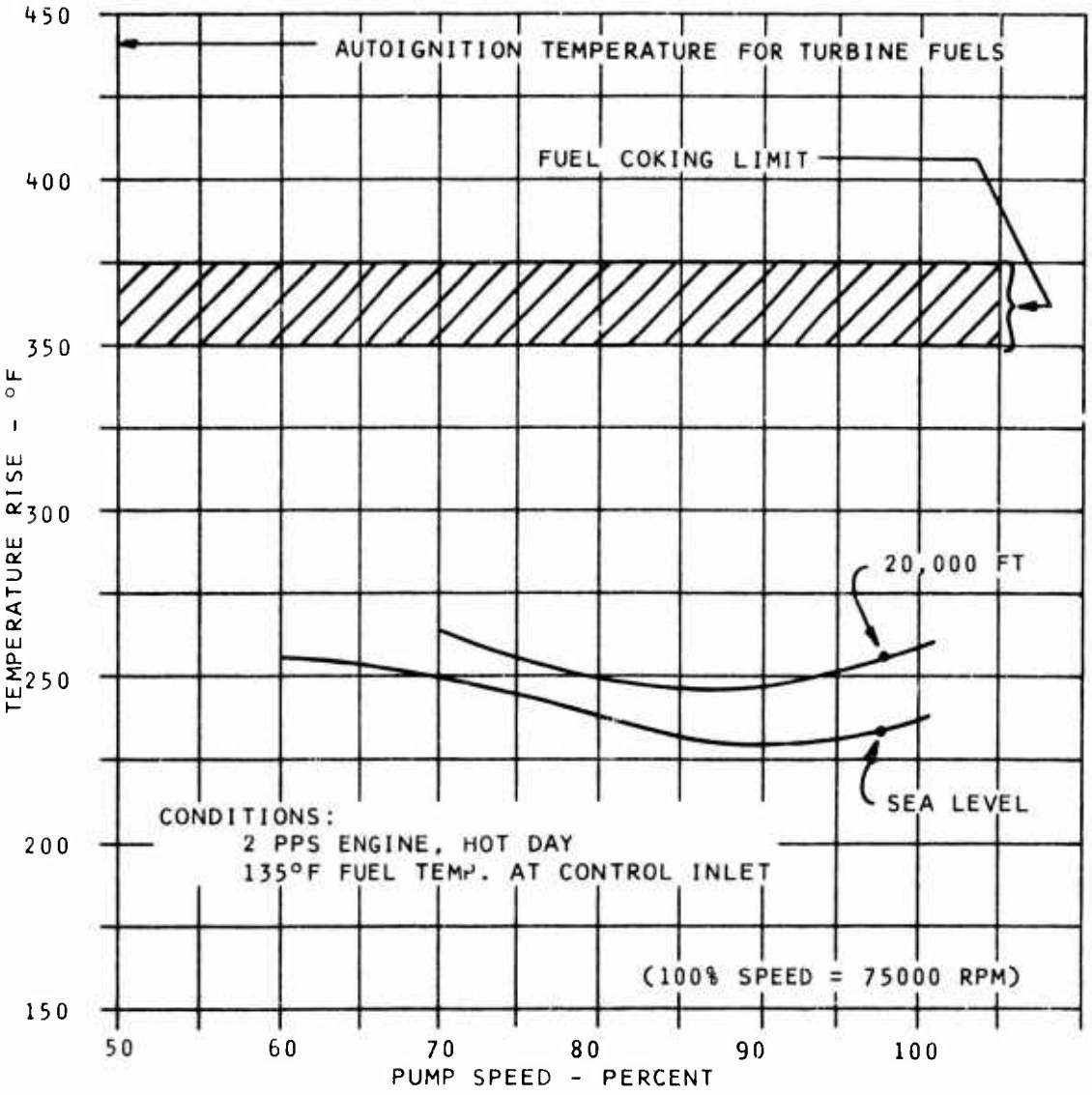

Figure 7. Maximum Steady-State Fuel Temperature, 2-PPS Engine - 75,000-RPM Pump.

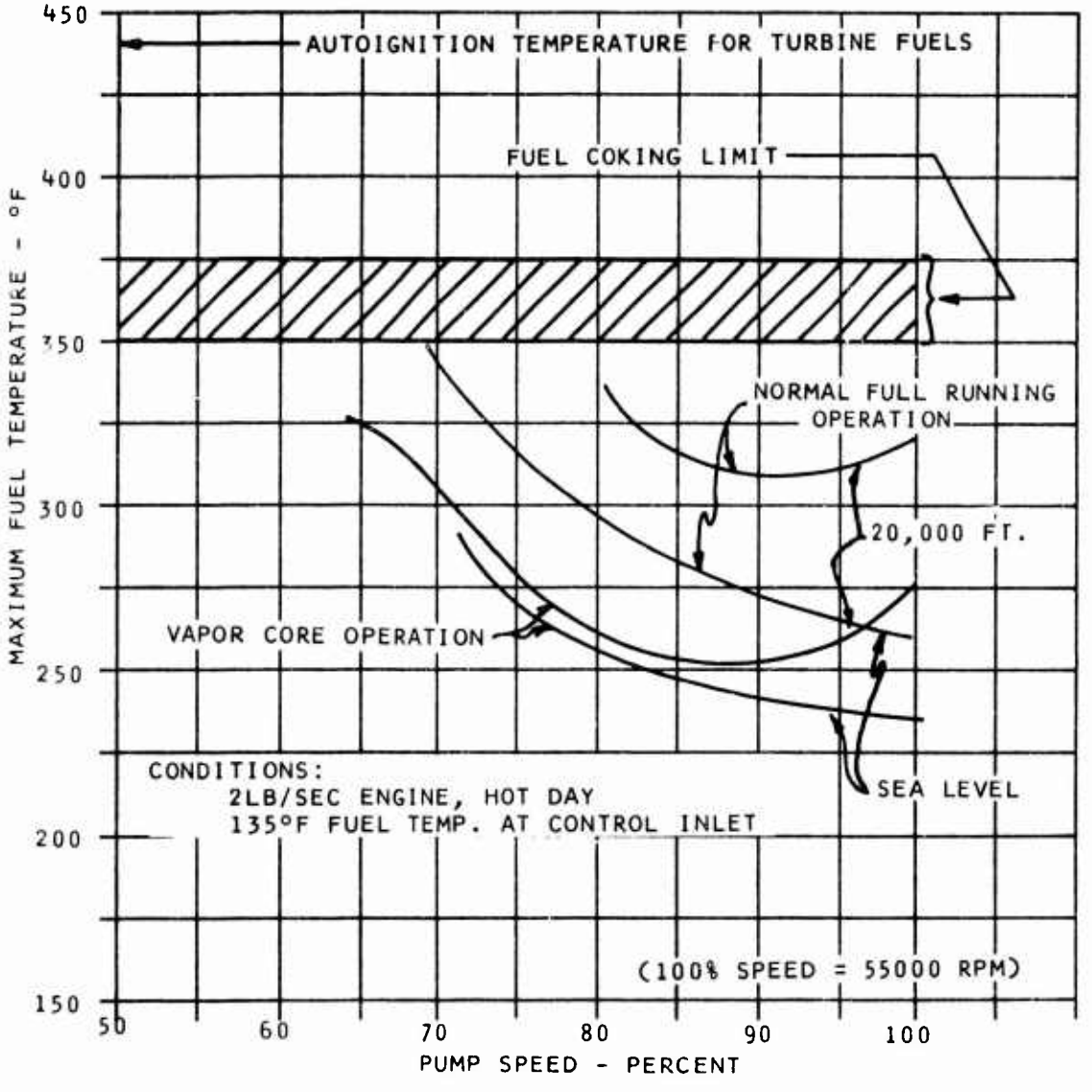

Figure 8. Maximum Steady-State Fuel Temperature, 2-PPS Engine - 55,000-RPM Pump.

10. It should be noted that there are physical problems introduced by operation at high speed. Bearings, critical speeds, balancing, and mechanical designs in general are more critical. The manufacture of small blades, the necessary tolerances required, and the effect of surface finish on notch sensitivity on a small shaft represent potential manufacturing problems. These problems have not been evident in this program due to the relatively short operation during these tests.

Discussion of Problems

The basic problem encountered to date in the development of centrifugal pumps is overall efficiency. The overall efficiency is defined as follows:

$$\eta_o = \frac{\text{Flow work produced}}{\text{Shaft work provided}}$$

The flow work is, of course, proportional to the flow rate multiplied by the pressure rise. The shaft work provided is equal to the sum of the following major work categories:

a. Flow work

b. Viscous friction work

c. Mechanical friction work

The viscous friction work is defined as that work which is done on the fluid minus the flow work output. The mechanical friction work is that work which is done on the seals and bearings of the pump.

To reduce the mechanical friction work, the seal and thrust bearing loads must be kept to a minimum. Achieving proper thrust balance producing minimum thrust loads was found to provide a marked increase in overall efficiency of the development pumps.

The major component of the viscous friction work is the impeller disc friction. In general, the disc friction work is

proportional to N^3D^5. The pressure rise across the impeller is proportional to N^2D^2. Therefore,

$$HP_{\substack{disc \\ friction}} \propto (\Delta P) \quad (ND^3)$$

By increasing the impeller speed N, the horsepower above would increase proportionally. However, a change in the diameter (D) has a much greater effect since it is cubed. So, in general, if it is desired to reduce the disc friction, the speed should be increased and the diameter decreased to give the same resultant pressure rise. This general assumption has proven to be true on these small, high-speed pumps. Also, the proportionality factor relating disc friction power and N^3D^5 is considerably greater than on higher specific speed pumps.

Another method of reducing the viscous friction work and flow work is to operate the pump in the vapor core mode. In this mode, the inlet of the pump is throttled, creating an inner vapor core in and around the impeller, as described in Reference 16. The pump thereby delivers only the flow and pressure which are required for engine operation. A conventional discharge throttled centrifugal pump provides discharge pressure which is essentially dependent on shaft speed only. So with the vapor core pump, both the required viscous work and the actual flow work are reduced. A decrease in overall power is expected and has been proven by test.

The fuel temperature data has been used to determine the maximum fuel temperature throughout the flight envelope. Figure 6 shows the maximum fuel temperature of the 55,000-rpm pump for the 5-pps engine. The flight conditions are sea level and 20,000 ft hot day with 135°F fuel at the control inlet. It can be seen that the pump meets the requirement for keeping the fuel temperature under the fuel coking limit of 350°F.

Discharge fuel temperatures will exceed the maximum allowable fuel temperature for the 2-pps engine if the same 55,000-rpm pump is used. The fuel coking limit is exceeded at speeds below 80%. If the pump for the 2-pps engine is driven at the same speed as the engine gas generator speed of 75,000 rpm

(at 100%), the maximum fuel temperature is reduced to within acceptable limits as shown on Figure 7. Hence, driving the pump at 75,000 rpm is a satisfactory solution to the high fuel temperature problem for the 2-pps engine. If the high drive speed is not available, vapor coring the 55,000-rpm centrifugal pump offers a possible solution. Figure 8 shows pump temperature rise for the 2-pps engine with the pump designed for 55,000 rpm operating in vapor core mode. Under these conditions, the ΔT is reduced to within acceptable limits. Figure 8 also shows a comparison of temperature rise for steady-state engine operation for the 2-pps engine using the 55,000-rpm pump with full-running operation and with vapor core operation.

Test Results

Preliminary test evaluation on a reworked impeller and volute housing, which had originally been sized to meet the 850 psi, 450 pph, and 37,500 rpm design conditions and was resized to operate at 50,000 rpm, resulted in the test data shown in Figures 9 and 10. This data demonstrated the improvement in pump temperature rise effected by the speed increase from 37,500 to 50,000 rpm. Figure 11 shows a photograph of both impellers.

At the completion of this series of tests, further testing at 55,000 rpm (the estimated 5-pps engine speed) was performed in an attempt to further reduce the temperature rise by operation at engine speed. To accomplish this, an impeller rework and new volute housing were required. The results of testing this unit are shown on Figures 12 and 13. Although these temperature rise curves are almost identical, the 55,000-rpm impeller produces a higher pressure rise at equal flow conditions and therefore it is more efficient than the 50,000-rpm impeller.

Results of vapor core testing of this 55,000-rpm unit are shown in Figures 4 and 5. The temperature rise at the required speeds and flows of the 2-pps engine allow operation at both sea level and 20,000-ft hot-day conditions without exceeding the coking limits of the fuel.

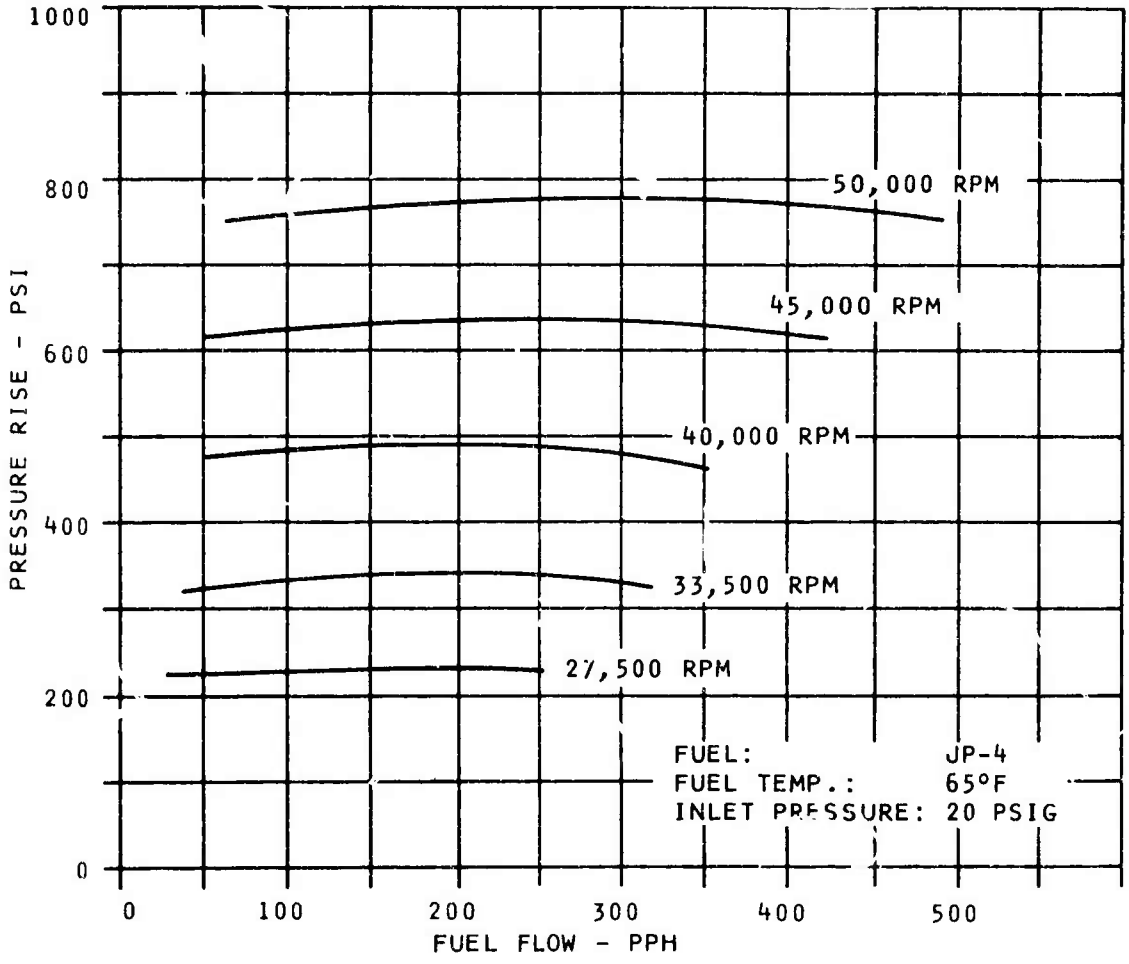

Figure 9. Pressure Rise vs. Fuel Flow for 50,000-RPM Pump.

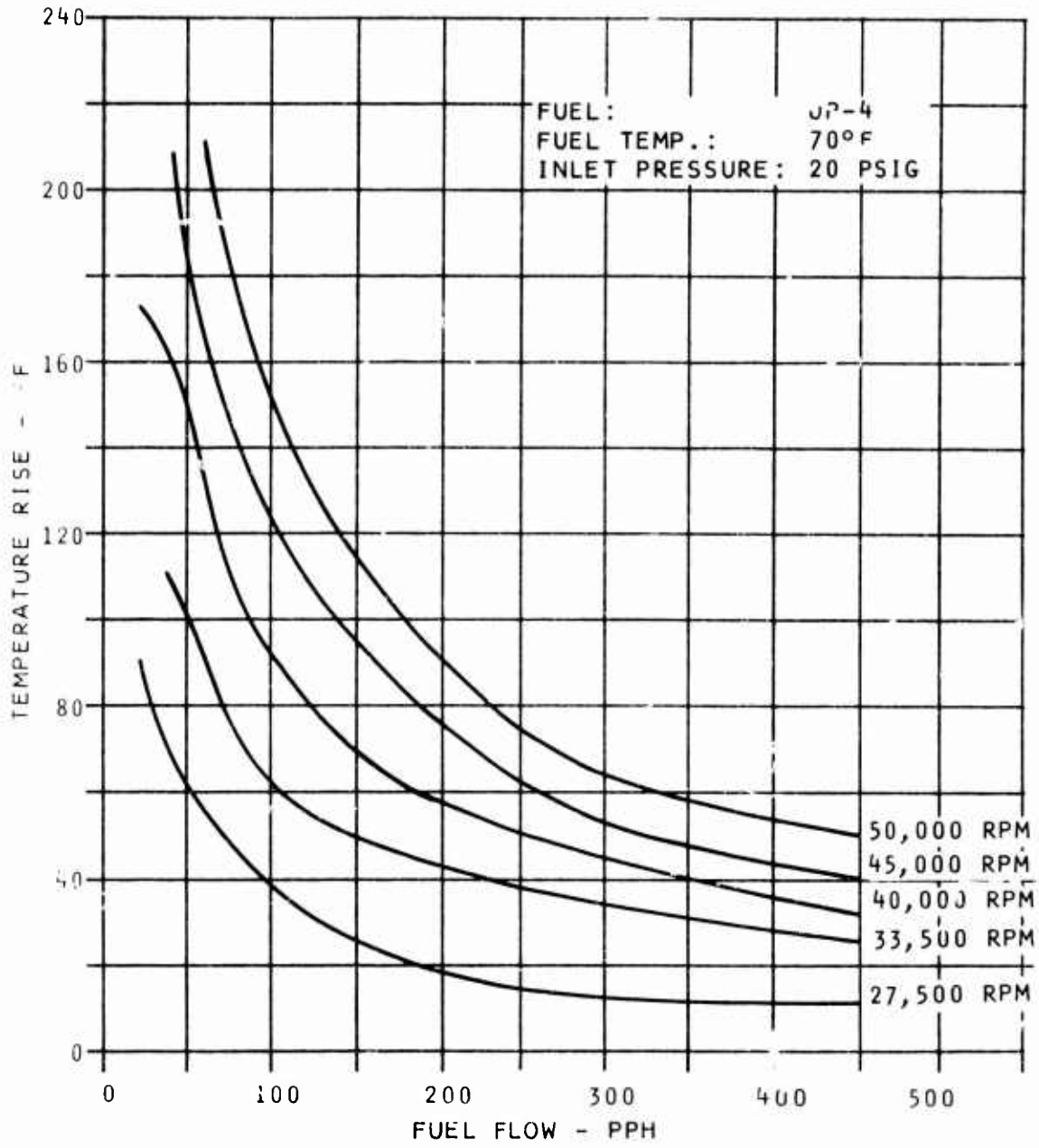

Figure 10. Temperature Rise vs. Fuel Flow for 50,000-RPM Pump.

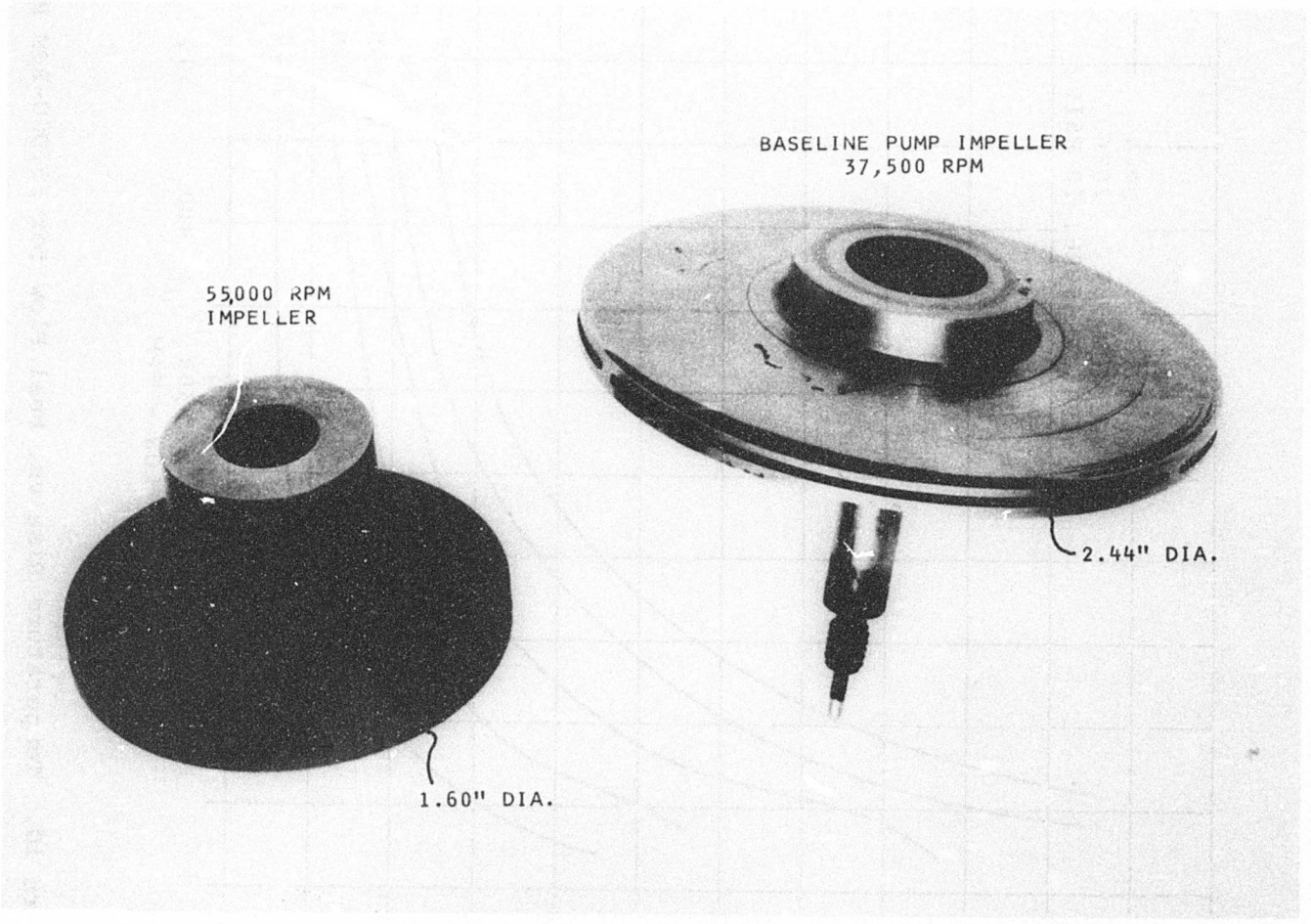

Figure 11. Fuel Pump Test Impellers.

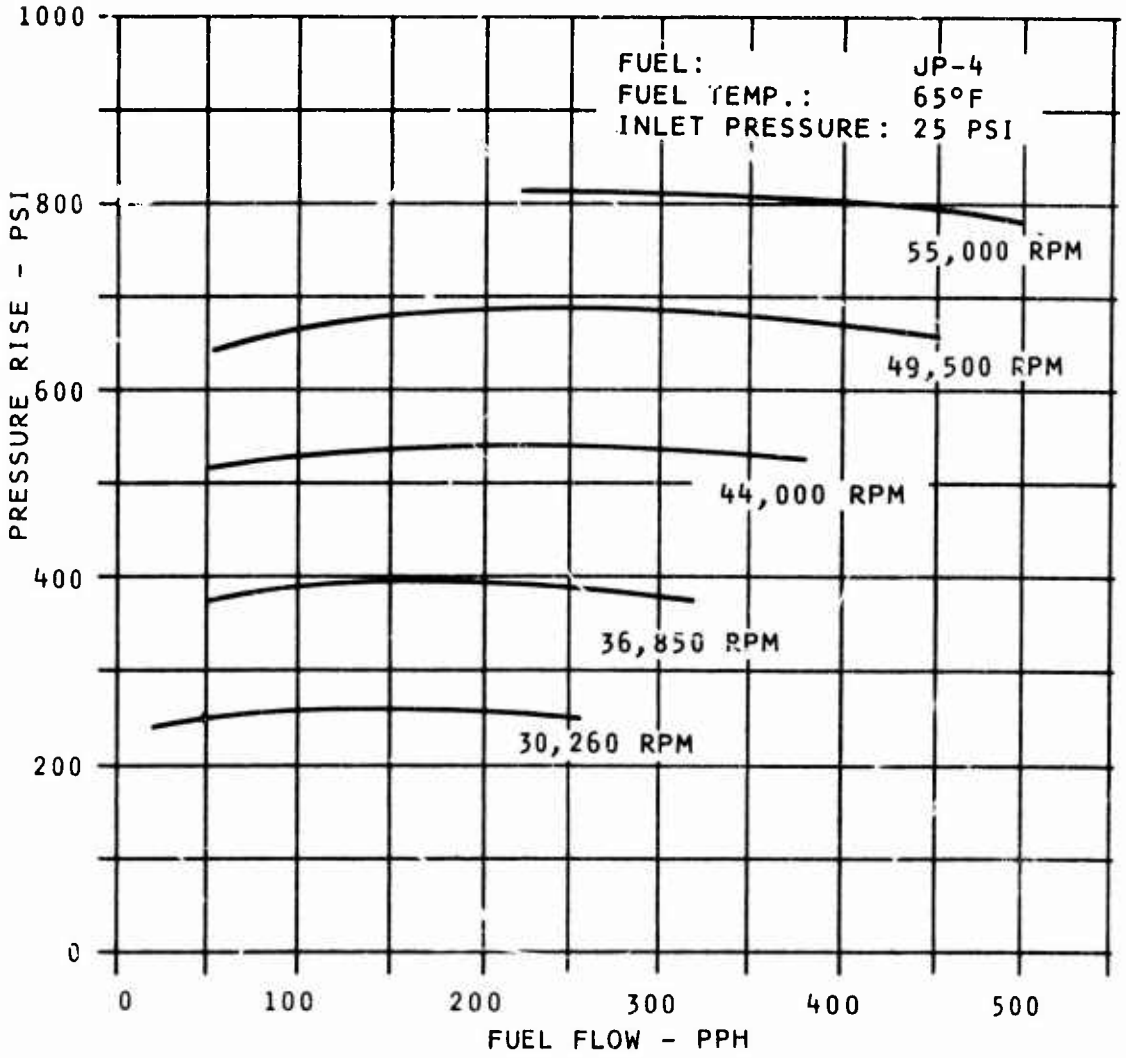

Figure 12. Pressure Rise vs. Fuel Flow for 55,000-RPM Pump.

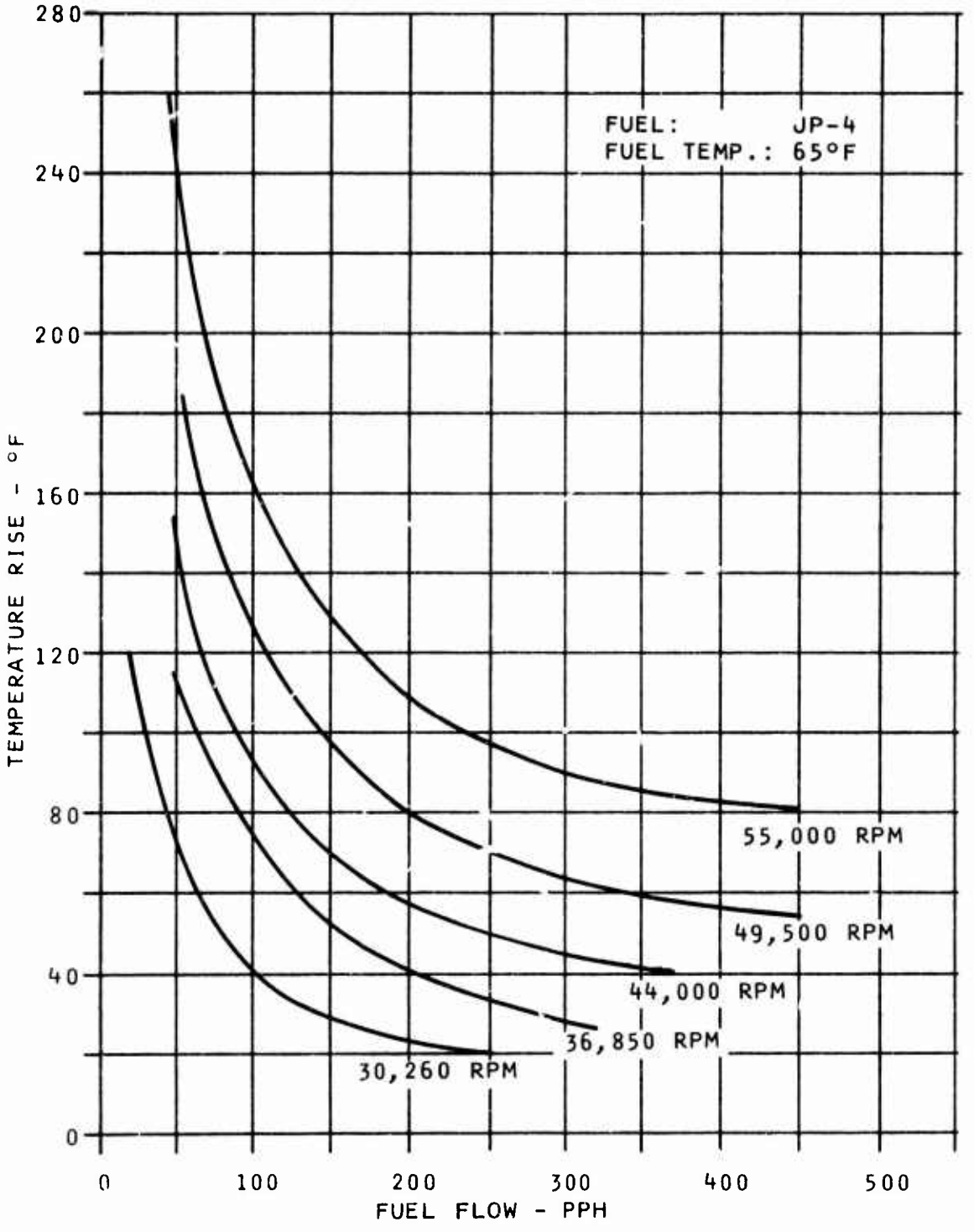

Figure 13. Temperature Rise vs. Fuel Flow for 55,000-RPM Pump.

ELECTRONIC COMPUTER

Electronic Computer Development

The original 30-month development program, referenced in the introduction, answered a substantial number of questions related to engine-mounted electronic controls and defined technical risk areas which required further development. The control power dissipation level of 60 to 70 watts, although not unreasonable for the control functional complexity, required an efficient convective cooling path to the fuel-cooled cold plate, and therefore the electronic computer was immersed in a dielectric fluid. Apart from an appreciable increase in the control weight, reliance on this fluid as a heat transfer medium has additional disadvantages, namely:

1. A leak could result in ultimate control failure due to overheating.

2. In order that all the printed circuit boards are covered with the fluid, over the flight attitude, it is necessary to completely fill the control. However, in doing this, some form of expansion chamber has to be provided to allow for thermal expansion of the fluid.

3. The dielectric fluid is relatively expensive.

A number of components within the control (hybrid circuits, Read Only Memory, voltage regulator output transistor, etc.) exhibited excessive power density. This condition provides a potential weakness,as any degradation of cooling could cause a thermal runaway condition.

Hybrid customized circuits can be split into two basic groups:

1. Those functions that are constructed from the customized development of a monolithic chip mounted on a substrate.

2. Those functions that are constructions from the interconnection of a number of standard chips mounted on a substrate.

Consultation with a number of customized circuit manufacturers has lead us to conclude that the reliability of the concepts

described under item #2 is questionable for application on gas turbine engine controls, and is basically due to the limitations of present-day technology. While the reliability of the monolithic approach referenced in #1 is acceptable, economic considerations prohibit their use, as production quantities in the thousands are required to make them a paying proposition.

However, manufacturing processes are improving; and should this result in either an improvement in the reliability of the concepts referenced in item #2 or the reduction in cost of those in item #1, then consideration would be given to their application to the control. The results of vibration testing indicated that potential problems existed and that the reliability of the control when exposed to vibration is extremely poor. Although the dielectric fluid offered a form of damping medium, subsequent testing of more viscous fluids has shown that this approach is inadequate.

It was, therefore, the initial intention of this program to address the aforementioned problem areas, to redesign those areas of the control concerned accordingly, and to prove the concepts by testing representative hardware. However, a brief review of requirements indicated that the program goals could best be accomplished by considering the complete control rather than only specific areas. Therefore, the program was undertaken to redesign the control and to build and test representative hardware to demonstrate solutions to the problems. Preliminary studies showed that problem areas would be resolved and reliability would be improved if the following design goals could be accomplished:

1. Reduce the total control power dissipation by a factor of ten by the incorporation of complementary metal oxide semiconductor (CMOS) components for digital functions and micropower components for analog functions, and by circuit redesign and simplification.

2. Eliminate the need for the dielectric fluid by the reduction of total power and elimination of hotspots.

3. Provide an environment such that the maximum temperature is 200°F and the maximum vibration level imposed on any element of the control is 30 g's.

Apart from these goals, it was also the intention to examine costly areas in the design and to consider alternative approaches in order that a cost-effective control could be provided.

Circuit Design

Low Power Concept

The primary cause of failure of the majority of electronic components is stress due to temperature. The sources of heat which cause a temperature increase are from ambient temperature and the internal electric power dissipated within the component. Limiting the surrounding air temperature requires a source of cooling as discussed in the section dealing with the thermal aspects of the design. Although military electronic components are rated for operation with a case temperature of 257°F, their reliability can be substantially improved by operation at lower temperatures. It was therefore decided that without the use of a dielectric fluid, 200°F should be our goal as a maximum component case temperature. To achieve this in the specified 250°F nacelle temperature environment, it is necessary to ensure that the self-heating effect of a component provides a negligible increase in the component's case temperature. To accomplish this, the majority of the digital and analog functions use CMOS and micropower components, together with their usual attendant passive elements. For areas that conventionally require higher relative levels of power and therefore potential self-heating problems, i.e., switching comparators, Read Only Memories, and actuator drive and power supply interface components, special provisions were made.

Digital Functions

CMOS was introduced over five years ago, and has since been developed into an extremely comprehensive product line. Within the past two or three years, many companies have developed their own and second source product lines. This factor, coupled with the prediction that within the next few years CMOS will be the number one digital logic family, should provide the most

economical approach. However, the main advantages of CMOS over alternative logic families are as follows:

1. Extremely low power dissipation, typically less than 1 mW per package.

2. Operation permitted over a supply voltage range of 3v to 18v.

3. Noise immunity specified as 45% of the supply voltage.

4. Potential of a significant improvement in component reliability because there is no self-heating.

Analog Functions

Micropower operational amplifiers are a relatively new breed of integrated circuit. Normally, with these components, an external resistor is used to set the quiescent power from 10 mW down to 1 mW (± 15v supplies). The trade-off at the 1 mW end, however, is a degradation in noise immunity and slew rate. The development of micropower operational amplifiers in the past few years has been possible due to the technology developed in the linear integrated circuit field. Input offset and bias parameters have been reduced, slew rates have been increased, and common mode and supply rejection ratios have been improved. As a by-product of these developments and the continued use of the field effect transistor (FET), it has been possible to raise impedance levels and still provide a component with good operating characteristics. To date, there are many companies that are offering micropower operational amplifiers, and the number promises to grow. Further, the low power concept provides for a very low power density level; in consequence, a number of companies are beginning to offer two and three micropower operational amplifiers in a single package. With further developments in this area, economical as well as performance advantages should be realized with the micropower approach.

Switching Comparators

In certain areas of the control it is desired to use switching comparators with slew rate capability approaching 30v/μs. With all micropower operational amplifiers, except relatively expensive models, testing has shown that 10v/μs is about all that is available with today's technology. Therefore, applications requiring fast slew rate will require a conventional switching voltage comparator. These devices, at a component case temperature of 200°F, dissipate approximately 80 mW, which is appreciably higher than their micropower counterpart. However, this situation can be tolerated as the number of applications requiring comparators are few, and by locating them on the printed circuit board to provide the optimum thermal conduction to the cold plate, their self-heating temperature rise will be minimized.

Read Only Memory

There is not presently available a low-power read only memory (ROM) suitable for application in the acceleration schedule. The ROM selected for this control has a maximum possible power dissipation which approaches 700 mW. Although the surface area of the ROM is appreciably larger than the majority of other elements in the control, the 700 mW would still present a significant power density, and the temperature rise, due to self-heating, would be unacceptable based on the present design philosophy. To alleviate this problem, the acceleration schedule was designed so that the use of the ROM was on a sample basis. This allowed for the ROM to be turned on only for short periods (≈3 μs), with the off time per cycle approaching 40 μs. With the ROM off, only a small standby power is drawn, and this, together with the short duty cycle "on" time, resulted in the ROM power dissipation reducing to approximately 60 mW, which will result in an acceptable self-heating temperature rise.

Power Interface

The power for the control is derived from the half wave rectification of a six-phase, permanent-magnet, regulated alternator. The rectification is performed by six diodes, each one dissipating 170 mW maximum. This power level is fixed by the current demanded by the control and its actuators and the voltage drop across the diodes. To prevent the occurrence of hot-spots and to limit their temperature rise, the diodes are mounted on a bracket which is mechanically connected to the cold plate, thereby providing a minimal thermal resistance between the diodes and the heat sink. A similar problem occurred with the stepping motor drive transistors. Although efficient switching current regulators are used for the stepping motors to minimize power dissipation, each of the eight transistors (four per stepping motor) dissipates an average power level of 180 mW; therefore, these components are located on the cold plate for efficient thermal conduction to the heat sink.

Crystal Oscillator

Temperature and vibration testing of the control during the prior 30-month development program revealed weaknesses in the crystal oscillator which was used as the heart of the control timing system. The problems were twofold:

1. Inadequate mounting of the crystal, resulting in failure when subjected to vibration testing.

2. Failure of the oscillator when subjected to a temperature of -65°F.

Although not specifically a problem, the oscillator did dissipate excessive heat and would not, therefore, conform to the present design requirements.

To alleviate these problems in the present design, a recently developed oscillator was purchased and incorporated within the control. This unit, which also includes the necessary countdown stages, utilizes CMOS, thereby providing an acceptable power dissipation level of 35 mW. A further feature of this oscillator is an improved method of mounting the crystal to provide immunity to the low temperature and vibrational problems encountered in the previous units.

Functional Design

Analog Versus Digital

Electronic gas turbine controls can be subdivided into four main sections: the power supply and its attendant regulators, the sensors and associated interface, the computation section, and the actuators and their required driving circuitry. For small gas turbine engine controls, the computation section normally accounts for only 25% of the complete control. Further, the performance requirements, taking into account operating conditions, are not nearly as arduous as that for other sections, such as the sensors and their interface. In consequence, although an all-digital control, on the outside, seems the desired approach, a closer look at all considerations yields a different conclusion.

In deciding upon the design philosophy for this control, the following factors were considered:

1. The accuracy requirements and operating conditions of the sensors are the primary limiting factor on system accuracy and performance. In general, they also present major elements in the cost breakdown of the control system. The selection of the sensors is, therefore, a major consideration in the design of the electronic computer and interface circuits.

2. Elements of the control demanding high accuracy, i.e., comparison of N_{ft} and N_{ftr} to 0.25% and

those areas requiring nonlinear functions, i.e., the acceleration schedule, are best implemented by digital concepts. An analog approach either would introduce unacceptable errors or would be too complex. A further variable is the choice between a continuous or a sampled data digital system. Each one has differing merits, and the choice between which one is used depends on the specific requirements. Within the control, both concepts were used, the N_{ft} and N_{ftr} comparison being an example of the continuous computation approach and the acceleration schedule of a sampled data concept.

3. Where extremely tight accuracy is not necessary and where either simple linear functions or dynamic compensation is a requirement, an analog approach is simpler and lower in cost.

4. A system that contains both digital and analog circuitry requires conversion circuitry to provide the interface from one format to the other. If care is not exercised, the required conversion circuits can become somewhat numerous and demand a certain degree of complexity. In consequence, care was taken in the design stage to minimize the number of conversions and to locate this interface in an area that allows for a simple approach.

5. The design of one section of the control must complement its neighboring functions. Care was taken, therefore, to ensure that a design simplification in one area did not cause a deferment or amplification of a problem in another area.

To summarize, therefore, the design philosophy of the control has been optimized to include a broad range of analog and digital concepts, with the specific design of any area reflecting a consideration for many important factors including economics, performance, response, flexibility, and complexity.

Standard and Customized Components

Although the majority of military electronic systems are manufactured using discrete components (resistors, capacitors, transistors, diodes, etc.) together with digital and linear IC's and MSI circuits, there is an ever growing consideration for the incorporation of customized LSI as a replacement for their standard component counterparts. During the previous 30-month program, a considerable number of customized hybrid circuits of the digital, analog, and power form were incorporated. However, this experience, together with consultations with hybrid circuit manufacturers, led us to the conclusion that we should avoid the use of customized circuits.

Although customized circuits offer volumetric advantages and may also provide marginal reliability improvements in some instances, there is a substantial nonrecurring cost involved in their development. Production programs with quantities in the thousands can most certainly take advantage of the customized concept as they have the volume to amortize the nonrecurring charge over the production quantity, thereby reflecting a minimal cost per component. However, the production quantity of a given airborne gas turbine engine control is not large and is spread over a number of years. So that even if the total quantity indicated a compatibility with customized circuits, with consideration for the total production time, the real possibility of modifications and the potential changes in technology, it is doubtful if a commitment to manufacture the total customized circuit requirement in one batch would be a wise decision.

A further factor that contributed to our decision to utilize only standard components was that more and more complex MSI functions, bordering on the complexity of LSI, are now being offered as standard products, and the trend promises to continue. Therefore, by using these MSI functions, the volumetric advantages offered by the use of customized circuits are somewhat negated.

Functional Description

Figure 14 illustrates a functional block diagram of the electronic control. The control provides all the functions included in the demonstrator control of the previous 30-month program and utilizes both digital and analog technology. Moreover, the control also includes the following additional features:

1. The N_{ft} error loop now incorporates a second-order lag instead of the previous first-order lag. Control mode studies indicated that acceptable performance can be obtained with a first-order lag dynamic compensation. However, performance can be substantially improved with the incorporation of a second-order system. With the previous all-digital philosophy, a first-order system is reasonably complex, but a second-order system is prohibitively complex. However, the present digital/analog design philosophy provides sufficient flexibility to allow the incorporation of the second-order system with a negligible increase in complexity over its first-order counterpart.

2. The N_{ft} loop integral reset concept developed during the previous program has been incorporated. This allows for the N_{ft} integrator to be controlled in a tracking mode, should any loop other than the power turbine speed be the controlling variable.

3. As with the previous program, the control will derive its power from a controlled alternator that is integral with the fuel metering section of the control. However, improvements have been made in this area, as follows:

    a. The alternator will provide power to the control and its actuators via a six-phase half-wave rectified winding. This concept allows for the maximum efficiency in the utilization of the available alternator

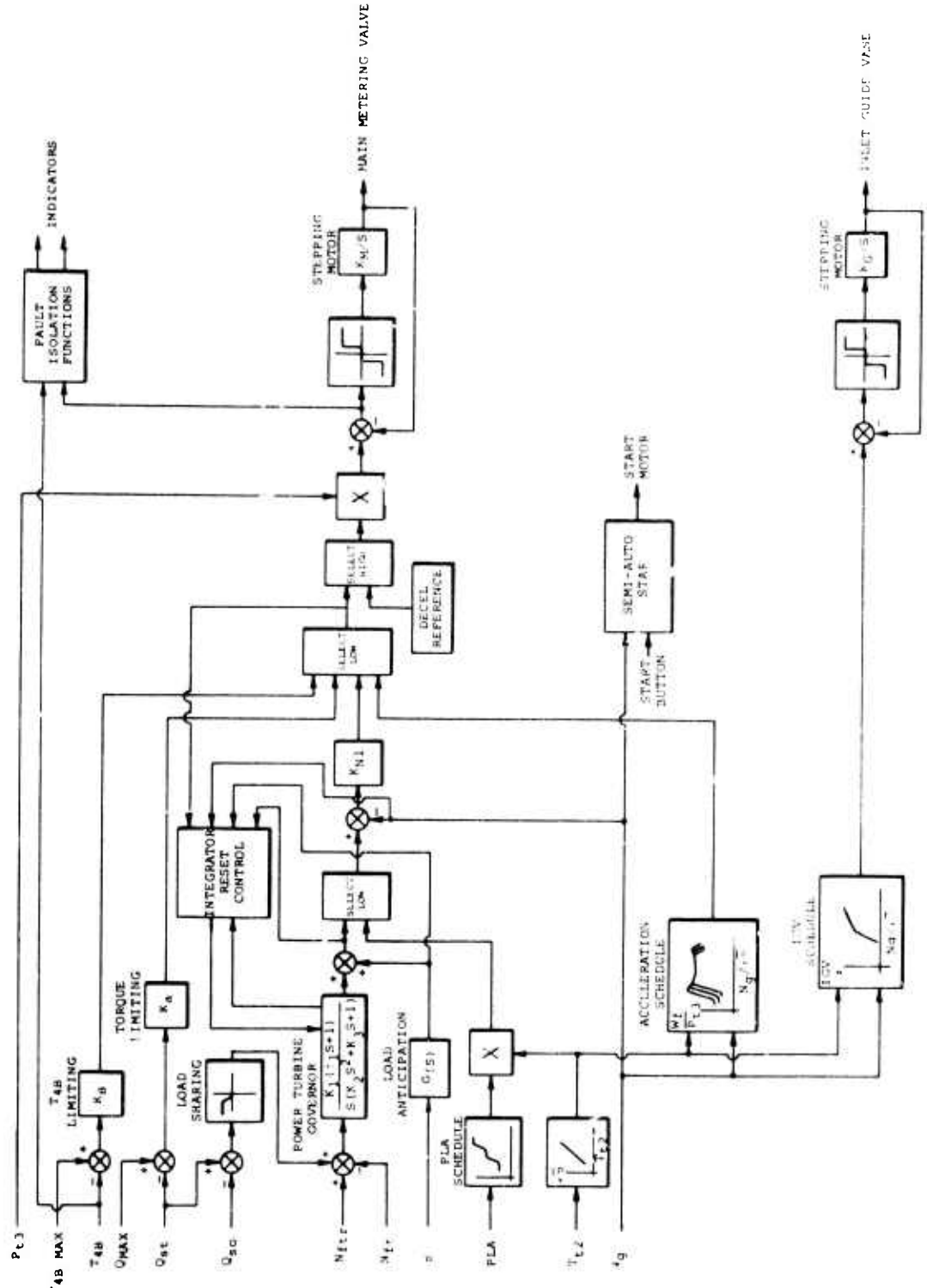

Figure 14. Computer Functional Block Diagram.

magnetic circuit. A further feature is that up to two windings can fail without degrading the performance of the control.

b. Instead of the alternator output voltage control being achieved with bidirectional variation of the current in the control winding ("bucking" to reduce the voltage output, and "boosting" to increase the voltage output), as was the case in the previous program, an all "boosting" scheme was used. This concept provides no additional problems to the alternator and allows a 75% reduction of the alternator control circuitry that is incorporated in the electronic control.

c. As a result of testing the alternator developed during the previous 30-month program, certain new and improved concepts are incorporated into the present alternator control circuits that will allow its output rectified voltage to be controlled to within ± 1.0v. This factor, coupled with a consideration for the extremely low power consumed by the control, permits the post alternator regulators, providing supplies for the analog and digital circuitry, to be of an extremely simple linear type. This compares with the previous arrangement that demanded the use of somewhat cumbersome switching regulators and their attendant potential EMI problems.

4. The provision of fault indicators to give maintenance personnel warning of a failure within the control is a very important requirement. It is, of course, necessary to be cost effective in providing this feature and to also ensure that reliability is not impaired. To satisfy this requirement, a preliminary study was conducted, and this evolved the following two concepts that were incorporated in the control:

a. The loss of the T_{4B} pyrometer detector or a fault providing an inhibition of light to the detector would provide the control with a large erroneous undertemperature signal, thereby allowing a blade overtemperature condition to occur. To ensure that the pilot is aware of such a condition occurring, a signal has been provided to activate a cockpit-mounted indicator. This signal is derived very simply by monitoring the presence or absence of an oscillating output from the T_{4B} detector first-stage current signal to voltage converter. The light emitted from the blades appears to the optical detector as an oscillatory signal whose frequency is proportional to the number of blades and the gas generator speed. This light signal, in turn, is converted to an oscillatory voltage whose amplitude is proportional to the maximum blade temperature measured. The failure detector then operates by monitoring this frequency. Should a gross failure occur, the output voltage could assume any level; however, it will be nonoscillatory. This condition is detected, and a failure indication is provided.

b. Under normal conditions the main metering valve position error signal has maximum known limits. Further, the most probable failure of any electronic component is to a hard-over condition, rather than a gradual degradation of performance. In consequence, should a gross failure occur in any control loop or the MMV position feedback circuit, it would most probably be reflected as a step or, at any rate, an abnormally fast change of demanded position (fuel flow). The position loop is rate limited by the response of the stepping motor; in consequence, a fast rate of change of demanded position would result

in an abnormally high position error signal. This condition, which at best indicates the gross failure of one or more control loops, provides an input to a cockpit-mounted indicator.

Although the aforementioned fault detection concepts are by no means all-encompassing with regard to any possible error, as a preliminary effort they do cover a large number of potential gross problems.

Performance Testing

During the design and assembly phases of producing the demonstrator control, careful attention was paid to the performance of each element of the electronic computer. The basic format of this testing was as follows:

Breadboard Testing Critical Areas

Breadboarded control functions were limited to the following critical areas:

1. Evaluation of CMOS to verify its low power capability, acceptance of a wide supply voltage variation, and to firm up the desired signal interface concept.

2. Evaluation of the different types of micropower operational amplifiers, with particular consideration for stability, input offset parameters and slew rate.

3. Circuits for use in the control including low power designs of an analog to digital converter, VCO, frequency comparator, and a one-quadrant multiplier. In all cases, performance and power consumption conformed to design constraints.

Individual Printed Circuit Board Testing

A test rack was constructed to enable the debugging and testing of all the printed circuit boards to be accomplished individually.

As well as room ambient testing, every board was briefly evaluated at approximately 180°F (by applying heat with a heat gun) to ascertain the stability of critical functions.

Complete System Testing

Test Equipment Used

Test Rig

In order that the printed circuit boards and other elements could be systematically integrated to form the complete system, a test rig was constructed that allows for the removal of the printed circuit boards without the necessity of de-soldering from the flexible interconnecting cable. This test rig is illustrated in Figure 15 and consists of an aluminum frame into which the boards slide. Connectors are provided between the flexible cable and the printed circuit boards, thereby permitting maximum testing flexibility. This rig was also used as a test vehicle for optimizing the physical shape of the flexible cables prior to manufacture.

Interfacing Cables

To provide adequate system noise immunity, cables were constructed to interface the electronic computer with all elements of the control. These cables included shielding concepts commensurate with the requirements of a typical engine application.

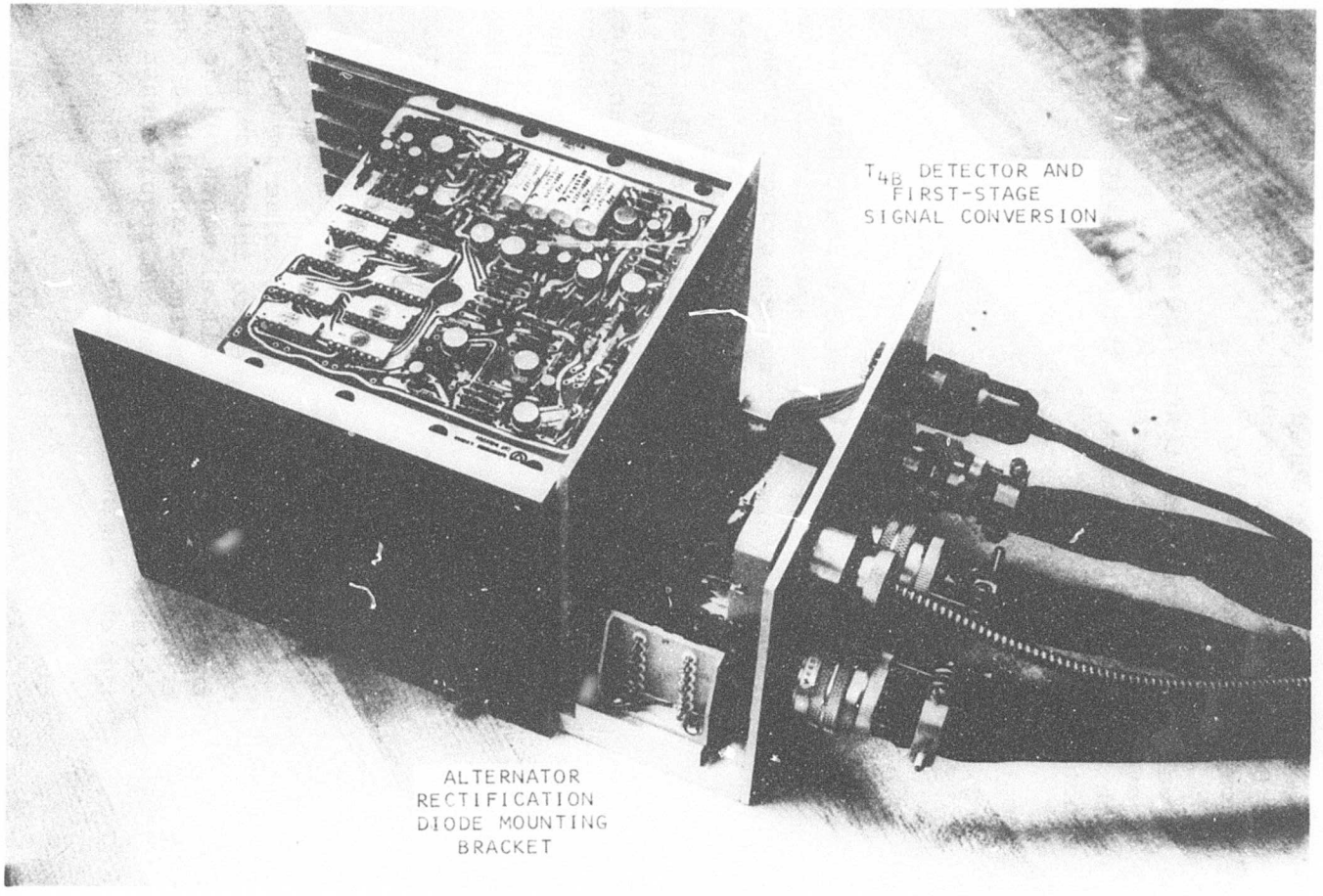

Figure 15. Electronic Computer Hardware Mounted in the Test Rig.

Control Test Set

Figure 15 illustrates a test set that was constructed to interface with the electronic computer. It provides simulated input signals that would normally come from the engine, cockpit, and fuel metering section of the control. Another feature of the test set is the provision of an interface to permit either open- or closed-loop testing of the electronic computer.

The program did not provide for an alternator, and therefore the input power to the electronic computer and the stepping motors is supplied from a ± 18 vdc supply. Potentiometers are used to simulate compressor inlet temperature T_{t2}, collective pitch β, and the free turbine reference speed N_{ftr} input signals.

Free turbine and gas generator speed signals are derived from VCO's, each one driving an isolation transformer to provide a reasonable simulation of the magnetic pickup signals. The PLA signal is derived from a resolver mounted in the test set and provided with a dial to indicate the angular position. An adjustable DC voltage is used for local and remote torque signals and also for the simulated compressor discharge pressure signal. Turbine blade temperature is simulated by an infrared, light-emitting diode driven from a current-regulated power oscillator. This arrangement provides a controlled, simulated blade temperature signal that is chopped to provide similarities to blade movement. A number of test points are brought out of the control and can be monitored with a digital voltmeter built into the test set.

T_{4B} and MMV position error, fault isolation function indicators are included in the test set, as is a feature that allows for the disconnection of the N_{ft} integral path so that open-loop calibration can be performed.

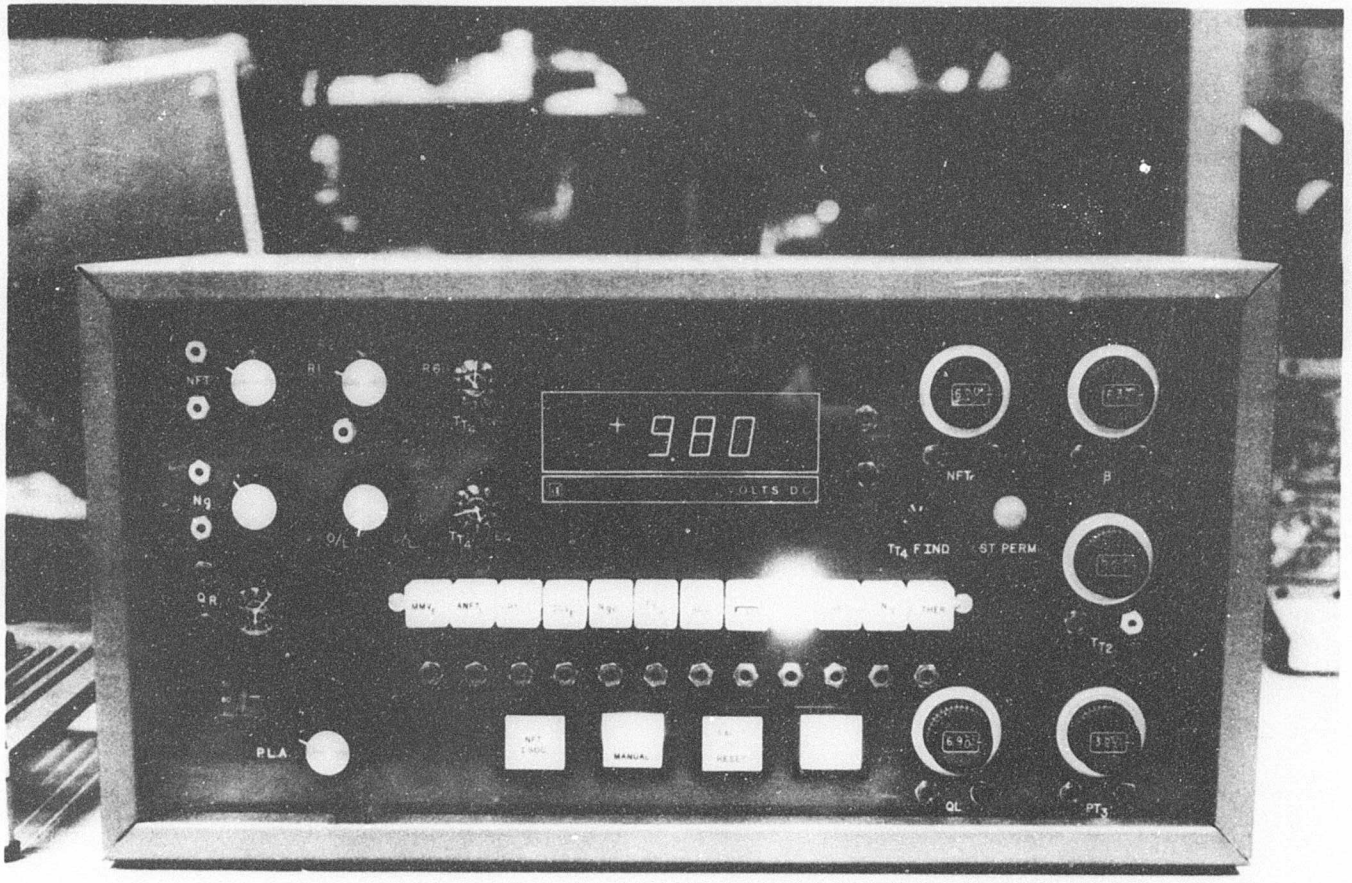

Figure 16. Electronic Computer Test Set.

Stepping Motor/Resolver Rig

Figure 17 illustrates the MMV and IGV stepping motor/resolver test rigs. The resolvers are geared with their respective stepping motors to achieve a 10:1 desired gear reduction. A ten-turn potentiometer powered from a stable voltage source is geared to the resolver and provides an accurate position measurement at different operating points.

Test Results

During evaluation and debugging of the control in the test rig, several problems arose that warranted corrective action:

1. The severest problem and most difficult to solve was that of random IGV and MMV stepping motor movement. The problem was traced to the stepping motors' current regulators that were coupling noise into the control circuitry. This problem was eliminated by incorporation of the following modifications:

    a. Improved shielding of external cabling connecting the stepping motors control and modification of these cables to eliminate unshielded areas.

    b. Improved filtering and stabilization of the ± 15V supply regulators.

    c. Modified stepping motor current return path on associated printed circuit boards.

    d. Incorporation of high-frequency filtering on the stepping motor drive transistors to minimize coupling effects between phases.

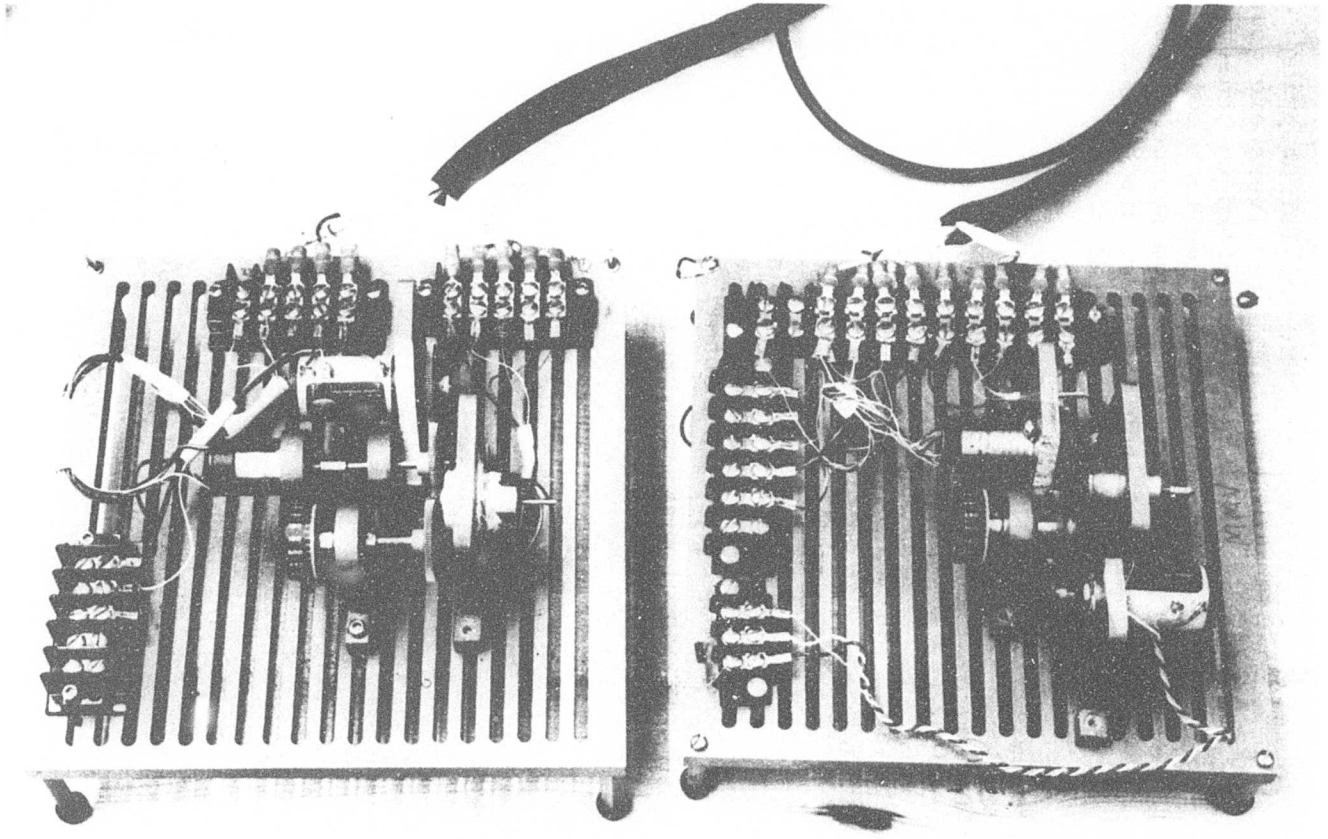

Figure 17. MMV and IGV Stepping Motor and Resolver Rigs.

2. The failure detection circuitry was found to load down the MMV position error signal. This problem was corrected by the incorporation of a simple buffer circuit.

3. The resolver circuits utilized for PLA, IGV and MMV functions exhibited jitter at one particular operating point. A marginal increase in hysteresis associated with the phase comparator circuitry solved the problem.

Having incorporated corrective action to eliminate these problem areas, the control was briefly exposed to an ambient of approximately 190°F to determine if any major thermal problems existed. After this successful testing, the electronic computer was disassembled from the test rig and reassembled into the demonstrator control package.

To evaluate the performance of the demonstrator control under worst-case conditions, the control was instrumented and put into the environmental chamber. Figure 18 illustrates the control with attendant coolant flow piping, electrical cabling, and bonded thermistors to monitor the temperature profile. The test equipment, connected to the control for environmental testing, is shown in Figure 19.

The environmental test program comprised testing at ambient temperatures of -65°F, +75°F and +181°F (all without coolant flow) and finally +257°F with coolant at +135°F and 36 pph flow. With all four conditions, the control was allowed to stabilize for a minimum of 5 hours to ensure that all components had come to temperature. In ascertaining performance variations, the +75°F (room ambient) calibration was taken as the reference, and the deviation with respect to this level was noted for the other conditions. The actual calibration procedure contained 14 parts, each part designed to evaluate the open-loop performance of a different element of the control.

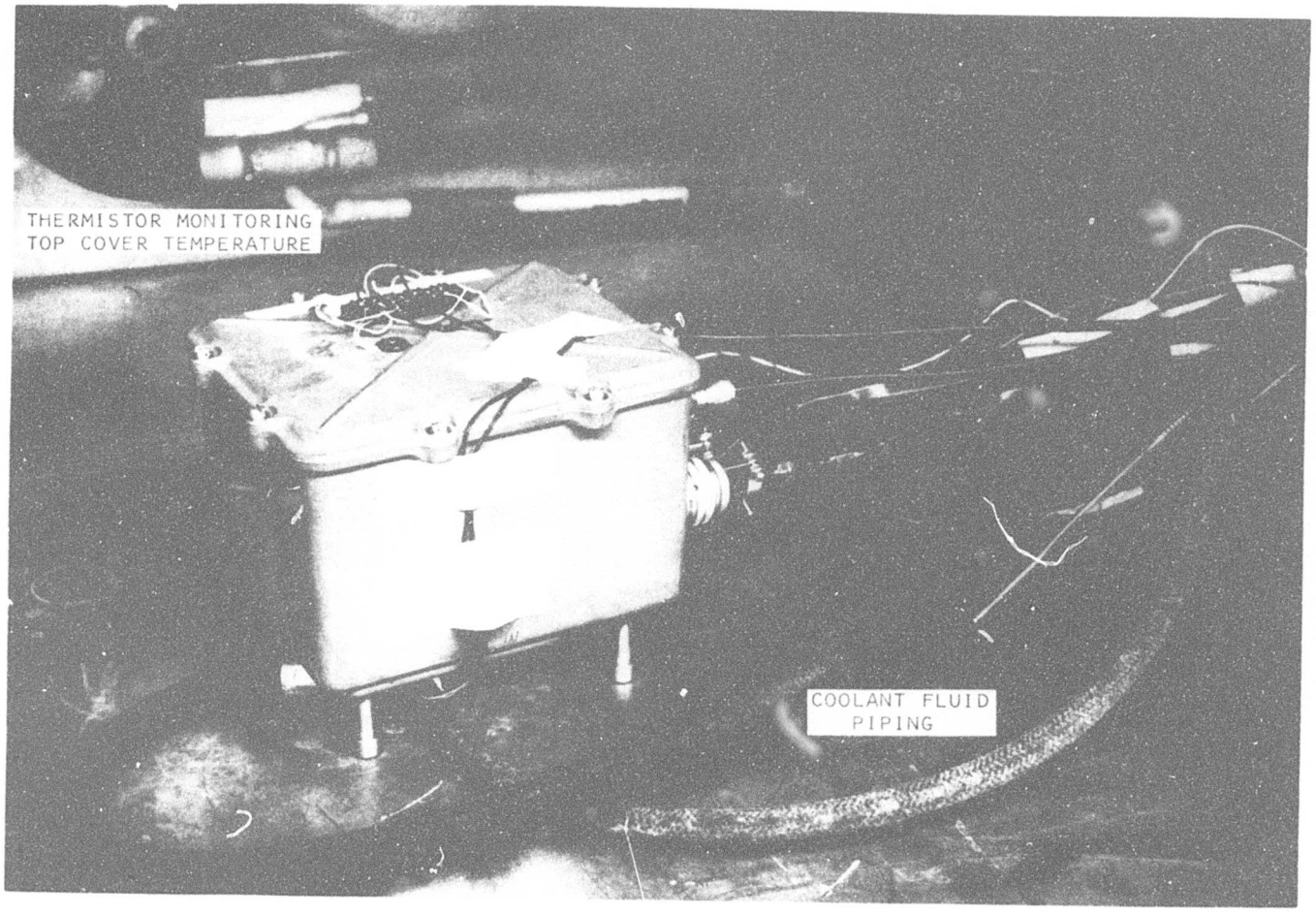

Figure 18. Electronic Computer in the Environmental Test Chamber.

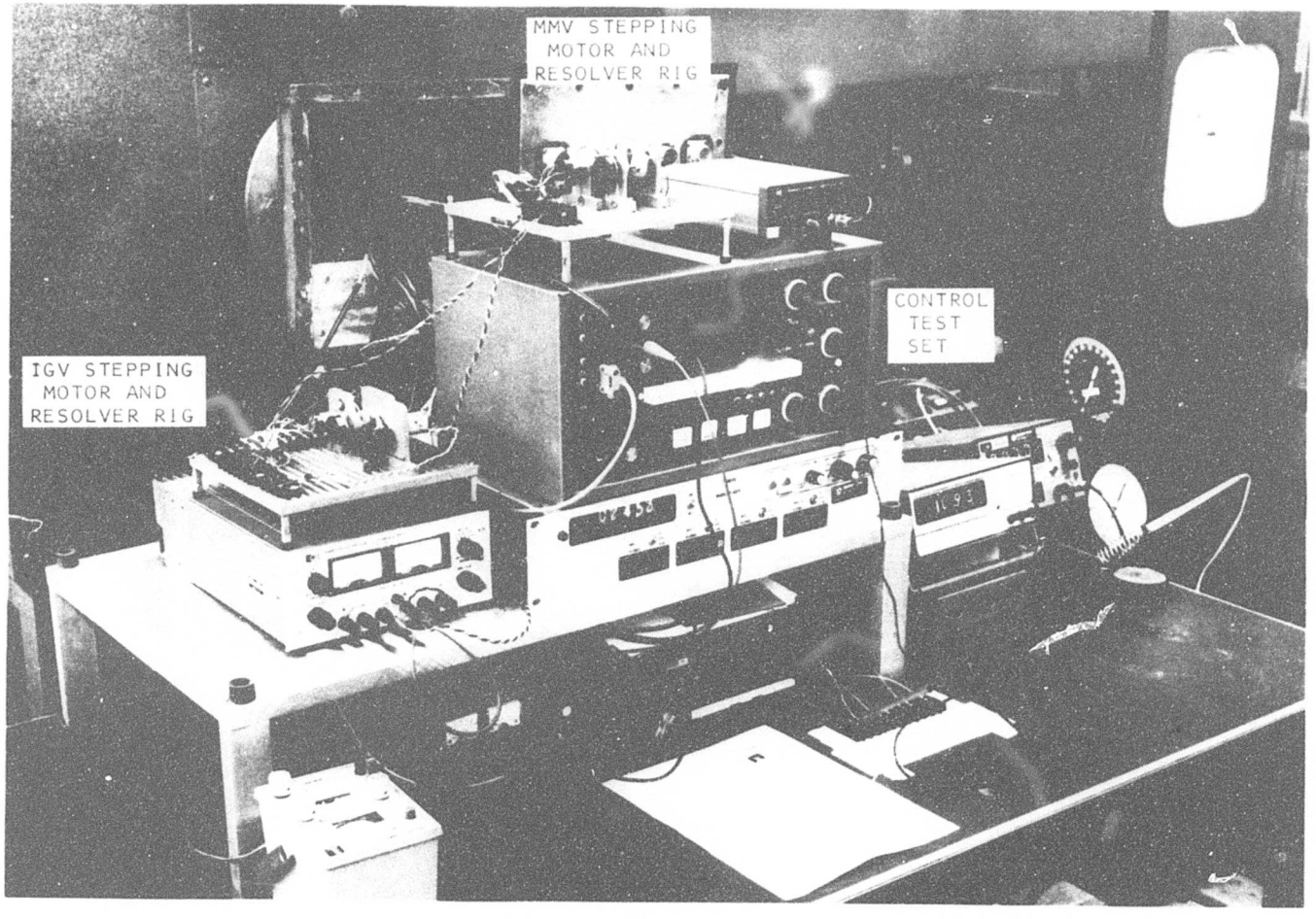

Figure 19. Electronic Computer Environmental Test Setup.

The results of this test program are as follows:

1. Throughout the entire test program, all elements were functional and there were no failures.

2. The output from the T_{4B} detector circuitry exhibited excessive change at the ambient temperature extremes. This, however, was predicted, as the characteristic of the optical detecting diode varies with temperature. Although the first-stage signal processing circuit has been designed to accommodate a thermistor/resistor temperature compensation network, this was not included because it is not critical to the goals of the program.

3. The gain of certain elements of the control (N_{ft} error path in particular) exhibited excessive change with variation in ambient temperature. In all but the case of the N_{ft} error loop, this problem can easily be rectified by the replacement of certain resistors with equivalents having improved temperature coefficients. With the N_{ft} error loop, the predominant problem lies in the digital to analog converter. The desired input signal should approximate a 50% duty cycle, whereas the actual duty cycle input is less than 5%. The inclusion of a single bit counter would allow an approximation to a 50% duty cycle, thereby negating the problem.

   It should be noted that even without correcting for the different gain changes, performance would still be acceptable on a closed-loop basis.

Power Dissipation Within the Electronic Computer

To determine the power dissipated within the electronic computer, each power supply and/or element of the control was monitored to measure the mean current drawn. From this, the power dissipated for that section was computed and the total from all sections was summed. The results are tabulated in Table II, and, as can be seen, the total power of 6.586W is within the 7W estimate. Although a pressure transducer has not yet been procured for the package, consultations with the pressure transducer manufacturer have resulted in the referenced power dissipation estimate being very realistic.

TABLE II. ELECTRONIC COMPUTER POWER DISSIPATION

Function	Power Dissipated (W)
MMV Stepping Motor Drive and Current Regulator	0.7
IGV Stepping Motor Drive and Current Regulator	0.7
+15V Supply (Analog Circuitry) Plus Regulation	1.776
-15V Supply (Analog Circuitry) Plus Regulation	1.188
+10V Supply (Digital Circuitry) Plus Regulation	0.284
+ 5V Supply (Digital Circuitry) Plus Regulation	0.114
- 9V Supply (Read Only Memory) Plus Regulation	0.12
P_{t3} Pressure Transducer (Projected Estimate)	0.48
Alternator Rectification Diodes (Design Estimate)	1.224
TOTAL	6.586 W

--- Packaging

As a result of performance, temperature, and vibration testing the demonstrator control developed during the previous 30-month program, it was noted that certain improvements could be made. The low-power dissipation concept of the present design has enabled these improvements to be augmented by additional features, resulting in a control package that has successfully addressed the important considerations of thermal and vibrational integrity.

Design Concepts

Figure 20 illustrates the layout of the electronic demonstrator control package. This package is an engineering demonstration unit. It is estimated that a production unit would be less than half this size.

The control consists of eight double-sided printed circuit boards (compared to the previous control's 13) that contain the majority of the components. These boards are shown by the photograph in Figure 21. Connections between the boards, connectors, sensors, and other elements of the control are provided by three printed flexible cables (instead of the four used in the previous design), and these are shown in Figure 22. Unlike the previous design, the printed circuit boards are mounted parallel to the cold plate. This arrangement, which is allowable by virtue of the thermal conductive cooling scheme utilized in the control, provides greater strength and minimizes differential movement when subjected to vibration. Also mounted to the cold plate are the stepping motor power drive transistors (via electrically isolating heat sinks) and a bracket containing the alternator rectifying diodes (shown in Figure 23). The cold plate itself is a very simple and inexpensive design which forms one side of a thin rectangular cavity. The other side of the cavity is formed by the base of the control housing. Inlet fuel is ported through the space between the cold plate and housing to provide cooling.

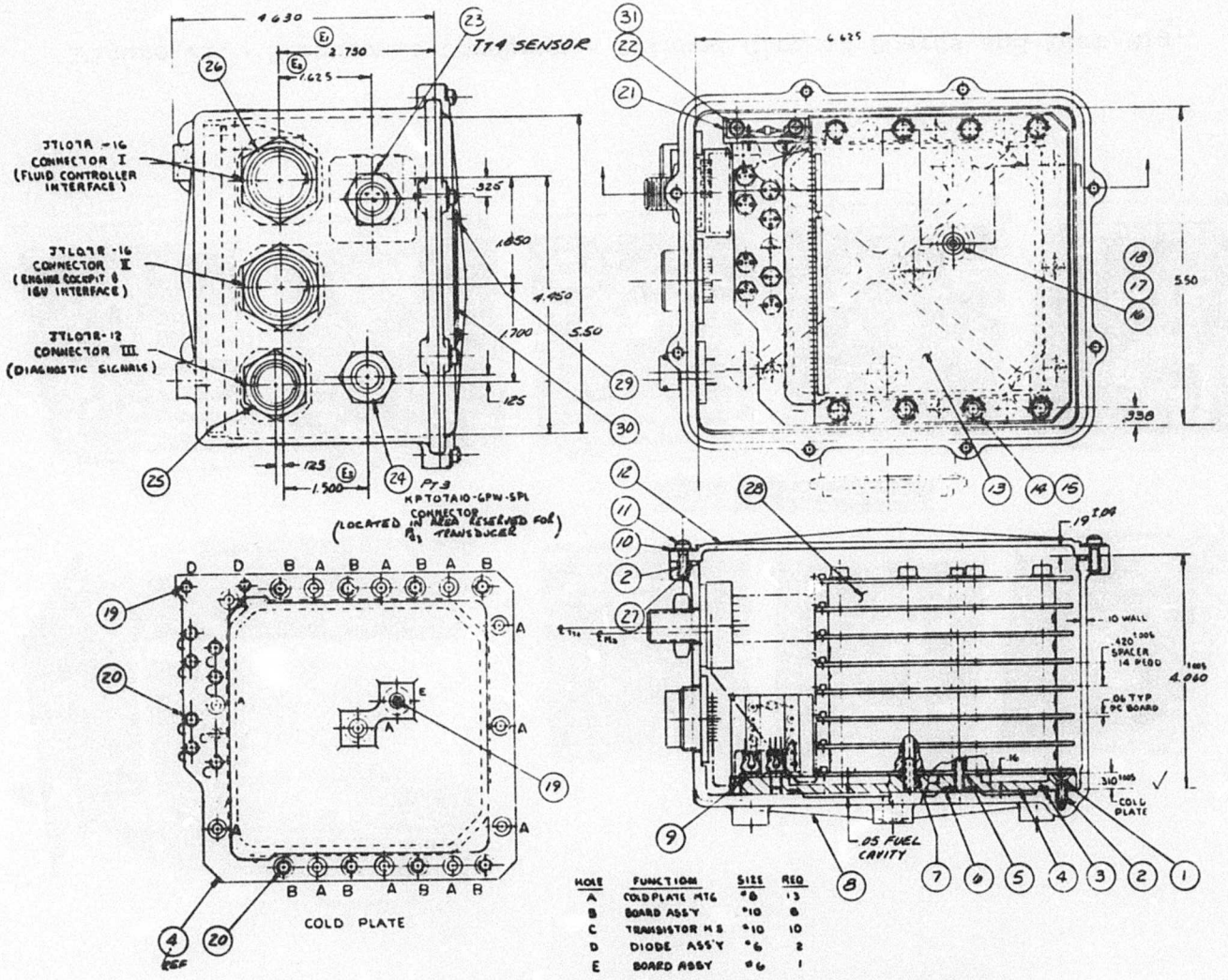

HOLE	FUNCTION	SIZE	REQ
A	COLD PLATE MTG	#8	13
B	BOARD ASS'Y	#10	8
C	TRANSISTOR H.S	#10	10
D	DIODE ASS'Y	#6	2
E	BOARD ASSY	#6	1

Figure 20. Electronic Demonstrator Control Package.

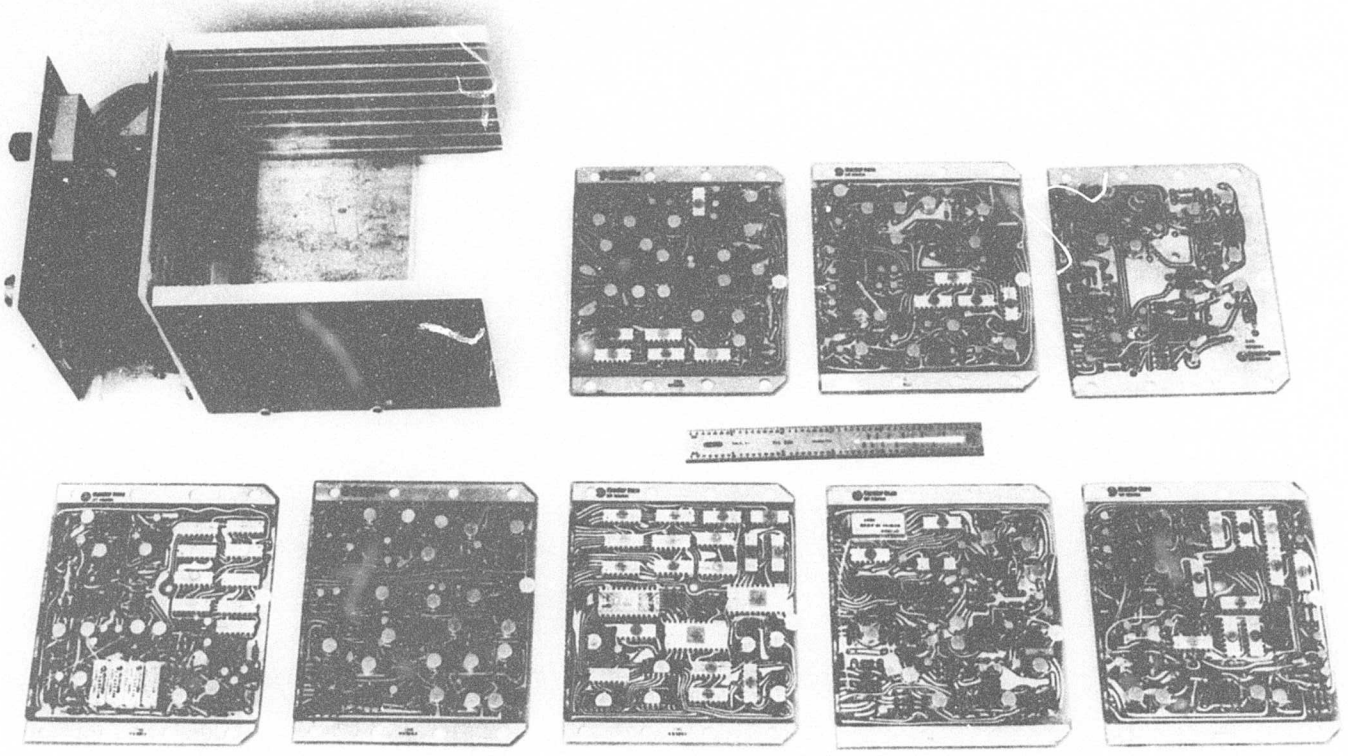

Figure 21. Electronic Computer - Printed Circuit Boards and Test Rig.

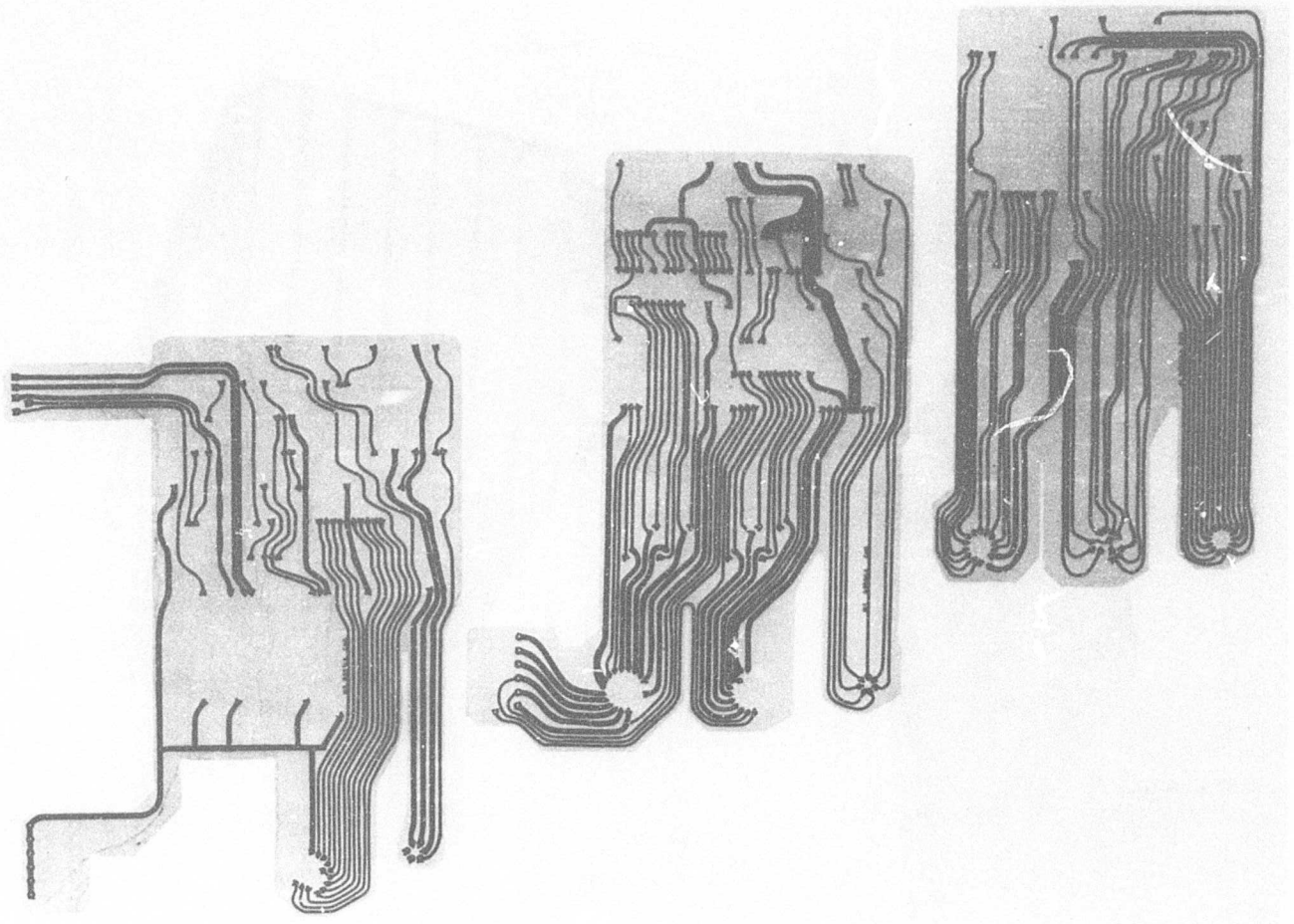

Figure 22. Electronic Computer - Interconnecting Cables.

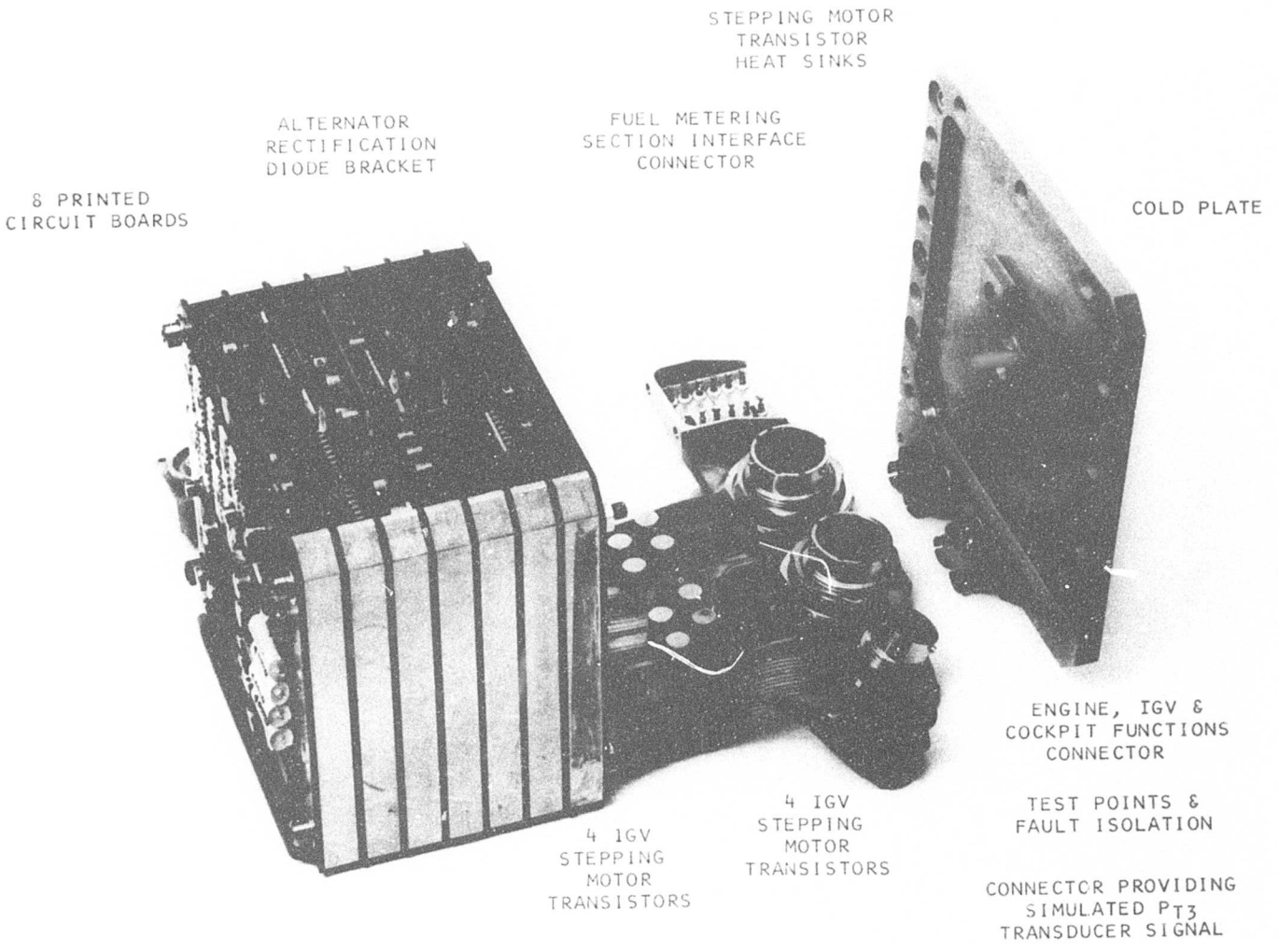

Figure 23. Electronic Computer - Internal Configuration.

The connectors are of a standard configuration, are hermetically sealed , and incorporate straight pins suitable for interfacing with the flexible cable. For the same reason, straight pins are also provided on the small T_{4B} sensor.

The design of the housing and the location of its elements show considerable improvement over its predecessor. All elements are attached to the flexible cables (as Figure 23 indicates) prior to assembly in the package, thereby providing a suitable configuration for ease of problem diagnosis and testing. Assembly itself is easily accomplished by the systematic location of each element in turn.

The housing is of a cast aluminum construction and was favored over a sheet steel construction for reasons of economics and improved strength.

Thermal Design

Development of the Thermal Cooling Concept

A primary goal of the program was to provide an adequate cooling concept such that the maximum case temperature of any component was limited to 200°F without the necessity of utilizing a dielectric fluid as a convective cooling medium. To achieve this goal and be cost effective, it was necessary to minimize the internal control power dissipation and to eliminate hotspots, thereby permitting the possibility of the success of a simple cooling scheme.

Having established that the total power dissipation would be about 7 watts, the control housing and cold plate from the preceding program were used as a test vehicle for experimentation of cooling concepts. Tests were conducted with and without the 7 watts power dissipation at worst-case environmental conditions of 257°F ambient temperature and with inlet coolant (silicone oil simulating fuel) at 135°F and 36 pph flow. Tests were conducted under these conditions to evaluate:

1. The thermally conductive coupling between the cover and cold plate.

2. Thermal isolation of the cover from the cold plate.

3. A thermal insulating lining (asbestos cloth) on the cover inner wall.

4. Variations of the coolant flow with conditions (1) through (3).

The results indicated that the control inside air temperature has a thermal gradient, with the low temperature being virtually equal to and adjacent to the cold plate, and that the maximum temperature occurs at the center of the cover, which is the point furthest from the cold plate. The results also indicated that the thermal lining, although providing a thermal lag, produced negligible improvement to steady-state conditions, and that the optimum configuration is item (1) above. With this arrangement and with conditions as referenced above, the "hotspot" air temperature within the control was found to be 192°F with no power dissipation and 207°F with 10 watts dissipated.

Analysis of these results, supported by further testing, revealed the following points:

1. Although the 192°F figure for the maximum air temperature is close to what we had theoretically predicted, our endeavors to reduce this level further by the increase in coolant flow were not successful, because the primary thermal resistive element in the loop from the hotspot air temperature to the coolant fluid is the thermal resistance of the cover and side wall. This resistive path could be reduced by either increasing the cover thickness or reducing the size of the control.

The former option would not be advantageous, as the control weight would be increased. However, design studies indicate that by the incorporation of modifications (use of multilayer printed circuit boards, circuit simplification, etc.), the control could be reduced in size by approximately a factor of two. This being the case, the primary thermal resistive path, referenced above, would be substantially reduced, thereby allowing the coolant fluid (fuel) to pull the hotspot air temperature below 192°F.

2. The 207°F air hotspot temperature with a 10-watt internal power dissipation presents a worst-case temperature rise. The 10 watts was provided from a small breadboard containing 40 resistors, each one dissipating approximately 0.25W. The mounting of the breadbcard provided a very poor thermal conductive path from the resistors to the cold plate, resulting, therefore, in air convective cooling being the only available effective mechanism. However, with the worst-case attitude of the control housing used during the test (cold plate at the bottom and cover uppermost), the convective path is from the resistors up through the air to the top cover, where conductive cooling takes over down to the cold plate. This convective path is, of course, valid only if there is a reducing temperature gradient away from the source. The net result, therefore, is for the heat source and the air between it and the top cover to be at a higher temperature than the cover. This situation, therefore, accounts for the 15°F air temperature rise from the unpowered to the powered case.

We concluded from these results that our objective of limiting the maximum component case temperature to 200°F was possible but that we would have to conform to two requirements:

1. The control should dissipate minimal power (10W or less), and it should be free of hotspots.

2. An adequate thermally conductive path must be provided from all components to the cold plate.

Our approach to the satisfaction of item (1) has already been discussed, and the solution to item (2) was developed as follows:

The thermal conductive path can be subdivided into two main parts: heat conduction through the printed circuit board and heat conduction from the board to the cold plate.

Printed Circuit Board Heat Conduction

The most effective thermally conductive printed circuit board is the aluminum cored board. This consists of an aluminum core over which is deposited first a thin insulating medium and then a layer of copper. The desired circuit pattern is obtained by etching away the unwanted copper. Holes for component leads, etc., are treated the same way, having first a layer of insulation, followed by a layer of copper. Thus with a component soldered in place, the only barrier between the heat conducted from the component via its leads to the aluminum core is a thin (.030 in.) insulating medium. Although this type of board exhibits excellent thermal properties, its relatively high production cost, questionable reliability (problems with shorts through the deposited insulating medium), and relatively poor permissible component packaging density make the use of such a board, with present-day technology, prohibitive.

The alternative, therefore, is the conventional glass epoxy printed circuit board, which, although not providing a thermal conductive path commensurate with the aluminum cored board, can do an adequate job if certain criteria are adhered to. By ensuring that the majority of the printed circuit board is covered with copper, and allowing the conductor to fill up all spaces, except for minimal spacing, by ensuring minimal power dissipation (approximately 0.5W per board) without hotspots, experimentation has indicated that the maximum thermal resistance from any component to the board interconnection pins is 19°F/W.

Heat Conductive Path, Printed Circuit Board to Cold Plate

The conductive heat path to the cold plate makes use of the flexible cables to conduct the heat from each board via its interconnections with the cables. This is achieved primarily by the ±15V, +10V, and signal ground conductors, which have been designed to have a minimum width of 0.05 in. (compared to the normal .025 in.) in both the boards and cables, thereby providing a substantial conductive path which can also enhance electrical performance. It should be further noted that all components utilized in the control in some way interface with one or more of the power supplies or ground system. On the eighth board (adjacent to the cold plate), the ±15V, +10V, and signal ground conductors have been arranged to have minimal clearance between themselves and an additional ground plane that is electrically connected to the cold plate via the printed circuit board interconnecting bolts.

It can, therefore, be seen that the only non-electrically conductive path to the cold plate is the minimal clearance between the power lines and signal ground path to the case ground plane on the eighth board. This arrangement

presents a thermal resistance that was estimated to be better than 30°F/W.

Based on the above-referenced configuration (which was designed into the demonstrator control), a thermal analysis was conducted. This analysis took into consideration worst-case conditions previously described with the addition that the 257°F ambient air was assumed not to be stagnant, but impinging on the control at a velocity of 40 feet per second, thereby providing a heat transfer coefficient of 0.035 W/in.^{2}°C over the package surface. Based on this data, the analysis indicated that the heat transfer into the cold plate from the effects of the ambient air was approximately 144W and that the "hotspot" component temperature (located in the center of the top board) will be less than 210°F.

Test Results

To evaluate the thermal concepts designed into the control, the electronic computer control housing and coolant system were instrumented with thermistors. As Table III indicates, fourteen temperatures were measured using thermistors. Six of these were located on the main printed circuit boards, one on the T_{4B} detector printed circuit board, three monitoring the control internal air temperature, two measuring the housing temperature, and two monitoring the coolant fluid conditions.

The location of the thermistors on the printed circuit boards took into consideration the desire to measure the temperature of the hottest components in the hottest locations.

The conditions evaluated were room ambient without coolant flow, 181°F ambient again without coolant flow, and 257°F ambient with coolant flow at 36 pph and 135°F inlet temperature to the cold plate.

A review of the results contained in Table III indicates the following points:

TABLE III. ELECTRONIC CONTROL TEMPERATURE PROFILE

Ambient Temperature (°F)	TEMPERATURE POINTS MONITORED														Test Conditions
	Th_1 (°F)	Th_2 (°F)	Th_3 (°F)	Th_4 (°F)	Th_5 (°F)	Th_6 (°F)	Th_7 (°F)	Th_8 (°F)	Th_9 (°F)	Th_{10} (°F)	Th_{11} (°F)	Th_{12} (°F)	Th_{13} (°F)	Th_{14} (°F)	
68	84	93	91	88	82	80	75	73	73	73	73	73			No Coolant Flow
181	190	190	188	188	183	183	181	181	179	189	189	181			No Coolant Flow
257	189	190	185	196	176	174	194	183	185	212	178	192	136	151	36 PPH Coolant Flow

Th_1	Operational amplifier located near the center of Board #1 (top board furthest from cold plate)
Th_2	Read Only Memory located on Board #3
Th_3	Crystal oscillator located on Board #4
Th_4	MMV stepping motor current regulator diode located on Board #5
Th_5	CMOS component located on Board #6
Th_6	Operational amplifier located on Board #8 (bottom board nearest to cold plate)
Th_7	Control air temperature furthest from the cold plate
Th_8	Control air temperature midway between top cover and the cold plate
Th_9	Control air temperature nearest to the cold plate
Th_{10}	Control housing, center of the top cover (point furthest from the cold plate)
Th_{11}	Control housing, on the side at a point adjacent to the cold plate
Th_{12}	Operational amplifier located on the T_{4B} board (rear of the T_{4B} detector)
Th_{13}	Coolant fluid into the cold plate
Th_{14}	Coolant fluid out of the cold plate

1. A primary goal of the program was to limit the case temperature of the hottest component to 200°F under worst-case ambient conditions. This goal has been met with the maximum temperature equalling 196°F.

2. With an ambient temperature of 181°F and no coolant flow, the maximum temperature rise is only 9°F above the ambient condition. This not only illustrates the success of the low power dissipation design but indicates that the control concept will be very suitable for applications whereby the electronic control can be mounted to the inlet particle separator where maximum ambient temperature is 135°F without the necessity of using coolant fuel.

3. Under all test conditions, the operating temperature of all components is very similar, thereby indicating the absence of hotspots in the design.

Vibration

The major vibration design problem in consideration of 20 g's excitation out to 2000 Hz per MIL-E-5007C is to provide damping for the PCB's to minimize induced resonant vibrations. Connectors used in the control are qualified to 50 g's, and the flexible cable connections between the PCB's and components are soldered in place and have a resonant frequency in excess of our range of interest. Electronic component pin connections are soldered, and the components are securely bonded to the PCB with a conformal coating. Although electronic components can be procured for operation in a 50 g environment, it was decided that as a design goal, induced vibration would be limited to 30 g's, to enhance reliability and reduce cost.

Providing PCB damping is the major design problem because of the inherently destructive high resonant amplitude characteristic of the glass-epoxy PCB in the range of specified vibration frequencies. Figure 24 shows the vibration characteristics of a PCB, of dimensions typical of a production

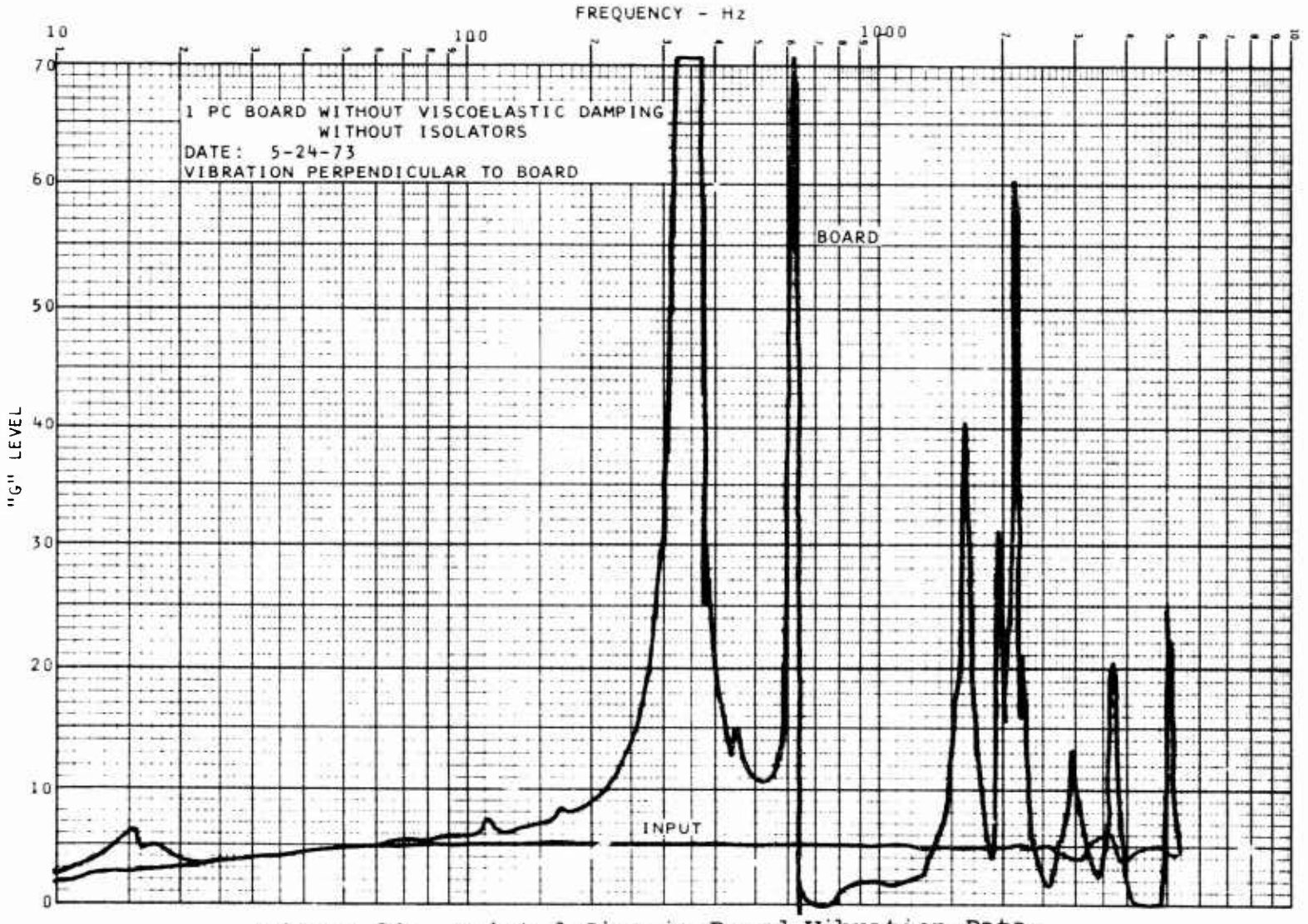

Figure 24. Printed Circuit Board Vibration Data.

design which was hard mounted to a vibration table by eight bolts, four each along parallel edges. The test results indicate a vibration transmissibility substantially greater than 14 and several resonant modes over the specified frequency range. The results of this test indicate the need for providing the PCB's with vibration isolation and/or damping.

During the previous development program, the crystal oscillator was the only electronic component which malfunctioned during vibration testing. Investigation indicated that the method used to mount the crystal in its package was not sufficiently rugged to withstand the specified vibration envelope. A new design was procured during the program and operated satisfactorily when subjected to a vibration level of 30 g's throughout the specified frequency range.

Design Studies

Analysis of PCB resonant frequencies indicated that they can be increased above 2000 Hz (the specification limit) by substantially increasing board thickness and/or decreasing board area. However, this approach leads to inefficient, costly packaging, and it was, therefore, discarded.

Filling the electronic package with epoxy was the simplest approach to the solution of the problem, and from past experience, this method would have a high probability of success. However, it suffers from the disadvantage of not allowing disassembly of the package for test or repair at the subassembly level and substantially increases the package weight.

Vibration isolation and damping could be provided either external to the package or internal. External isolation and damping is provided by mounting the package on vibration isolators. It is a common approach to solving vibration problems in practice, and it has the advantage of ensuring that all components and subassemblies in the package are protected against vibration.

The electronic package was analyzed to compute the spring rate and damping required in the vibration mounts to provide the required vibration isolation. The analysis was done by representing the dynamic properties of the PCB assembly by an equivalent undamped spring/mass system coupled to a damped spring/mass system representing the rest of the package plus the vibration mounts. The entire spring/mass system is coupled through the vibration mounts to a vibrating plane representing the engine; vibration is considered restricted to translatory motion in the worst-case direction only (normal to the PCB's). The model described above was analyzed to compute peak board deflection, component acceleration, and housing displacement, for an optimum vibration isolation. The results indicate that optimum isolation is obtained when the vibration mounts are selected to tune the system for resonance at 54 Hz. For this condition the PCB component acceleration would be 20 g or less. This result is approximate, but is sufficiently accurate to specify the requirements for the vibration mounts.

Two leading manufacturers of vibration mounts were contacted. One is a leader in elastomer type mounts and the other a leading manufacturer of helical spring type mounts. Both confirmed the results of our analysis and recommended vibration mounts which meet the requirements for optimum response. Both manufacturers proposed mounts that were rather large and which would significantly increase the height of the fuel control. In addition to this problem, other major difficulties included:

1. The requirement for flexible tubing to carry fuel in and out of the cold plate. This tubing could experience a fatigue failure and reduced reliability due to the vibratory motion of the housing.

2. Elastomer type vibration mounts require materials which are not vulnerable to fuel oils, and this requirement is incompatible with optimum elastomer damping properties.

3. Helical springs are unable to provide uniform vibration isolation and damping for all directions of motion; also, their damping is low for large vibration amplitudes.

4. Elastomer type mounts which can withstand JP fuels have limited life due to wear and must be replaced after 800 hours of operation.

Because of the many disadvantages inherent with this concept, the possibility of providing the electronic package with internal vibration isolation and/or PCB damping was considered. The following techniques were evaluated:

1. Internal structural damping of the PCB's by bonding a viscoelastic material 0.070 in. thick, which covers the underside of the PCB.

2. Viscous damping of the PCB's by filling the electronic package with a silicone viscous fluid of 10,000 centistoke viscosity.

3. Individual encapsulation of each board in the assembly with a resilient potting resin so that all voids between boards are filled.

4. Internal vibration isolation.

Preliminary testing was conducted on five of the demonstrator PCB's with mounting identical to that to be used on the demonstrator control. Vibration levels were measured at the center of the middle board, and all testing was conducted without components on the PCB's. This was considered to be acceptable, as the testing was mainly a comparison of different damping concepts, and prior evaluation had shown that the only difference between a PCB with components and one without was an approximate 20% change in resonant frequency. Testing was conducted mainly in the axis normal to the PCB's, as this presents the worst-case conditions for both the PCB's and their associated components. Although the vibration specification calls for the "g"

level to increase to 20 g's at 460 Hz to 2000 Hz, a constant 5 g level throughout the range was used in the majority of this evaluation test program.

Test results showed that the viscoelastic material limited the resonant amplitudes to less than 10 to 1 transmissibility in the specified 5 g range (20 to 460 Hz) and to less than 7 to 1 over the 20 g input frequency range (460 to 2000 Hz). The damping provided by this method was considered to be too low, as the desired 30 g maximum limit was exceeded in both the 5 g and the 20 g ranges.

The vibration response of the PCB's when they were immersed in the viscous fluid medium showed satisfactory damping at the frequencies below 500 Hz, but the damping was not sufficient in the high-frequency range, particularly at frequencies near 2000 Hz.

The vibration response of the encapsulated PCB assembly indicated satisfactory damping below 500 Hz and a significant improvement in damping over the 500 to 2000 Hz frequency range with a maximum transmissibility of about two. This technique offered the best approach to providing satisfactory external damping for the PCB's over the entire vibration frequency range (20 to 2000 Hz). However, the desired 30 g limit would still be exceeded in the high-frequency range.

Studies were made of various possible methods of providing internal vibration isolation. The design philosophy, as was the case for the external vibration isolation concept, was to provide an isolation system with a low enough resonant frequency and amplitude to attenuate all of the PCB's resonant frequencies to below the 30 g level. The resultant designs were excessively large. Further studies indicated that the isolators could be reduced to a reasonable size if they were used in combination with one of the PCB damping concepts. The best overall combination in consideration of cost, weight, flexibility and simplicity was judged to be isolation and PCB damping using viscoelastic material. Figure 25 shows an

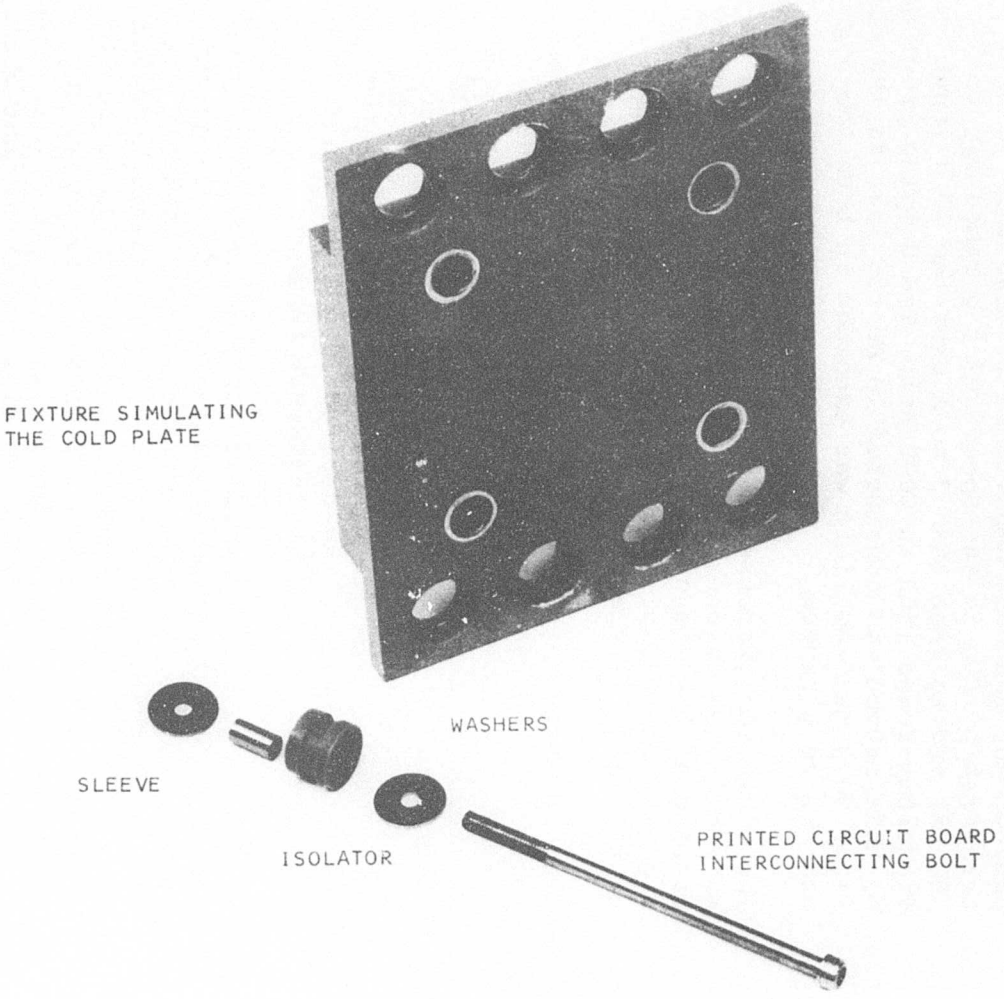

Figure 25. Vibration Isolator Test Configuration.

exploded view of one of the isolators, and Figure 26 depicts a PCB with the viscoelastic material bonded to it.

The elastomer isolators are manufactured of a silicone base material. The isolator will be located inside the electronic control and will therefore not be subjected to fuel. The estimated design life is 5000 hours. The isolator and viscoelastic material are qualified to operate at a temperature range of -65°F to +200°F, which is consistent with the environmental temperature range inside the electronic control.

Test Results

A complete evaluation of the combination of viscoelastic PCB damping and vibration isolation was completed using a five PCB assembly as illustrated in Figure 27 Prior to evaluating the complete assembly, the vibration characteristics of an untreated PCB were established by vibrating one board which was hard mounted by eight bolts to the vibration table. The results of this test were shown in Figure 24. The next test series was done to establish the vibration characteristics of a PCB with the viscoelastic material bonded to it. The results are shown in Figure 28 and indicate a slight increase in the fundamental resonance frequency due to the addition of the viscoelastic material and a substantial attenuation of all of the resonant modes.

The five PCB test assembly has provisions for mounting eight vibration isolators. The eight isolators were designed in consideration of the prototype eight PCB assembly with mounted electronic components. However, to establish that the selected design would work, it was not necessary to duplicate the prototype eight board assembly, and by limiting the vibration test set-up to five PCB's, hardware fabricated for the prototype unit could be utilized. A series of vibration tests was conducted on the five board assembly, starting with all eight vibration isolators. The number of isolators was reduced to four to lower the fundamental frequency to the 100-Hz range. This frequency

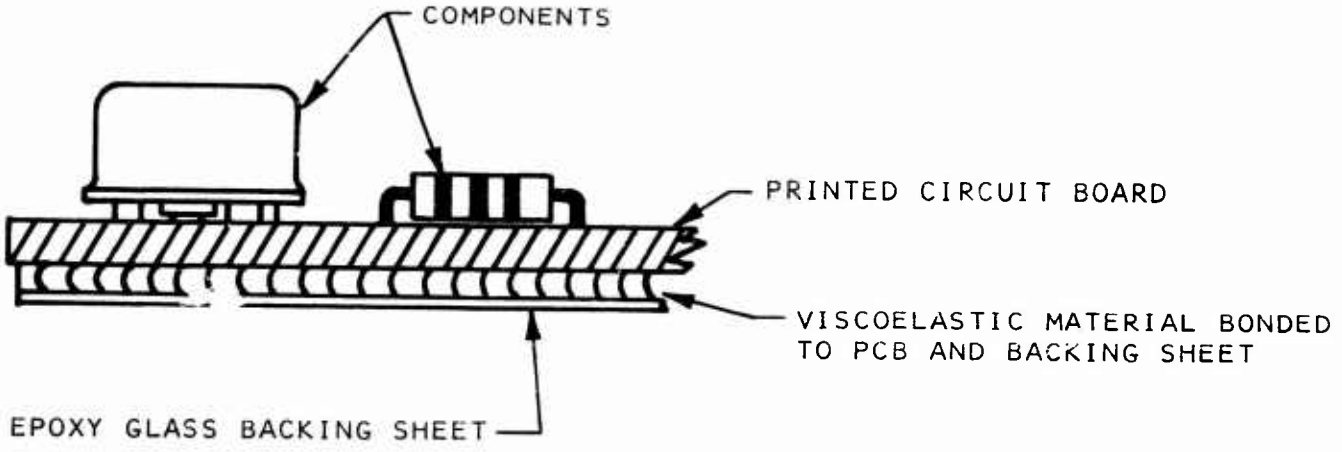

Figure 26. Configuration of Viscoelastic Damping Concept.

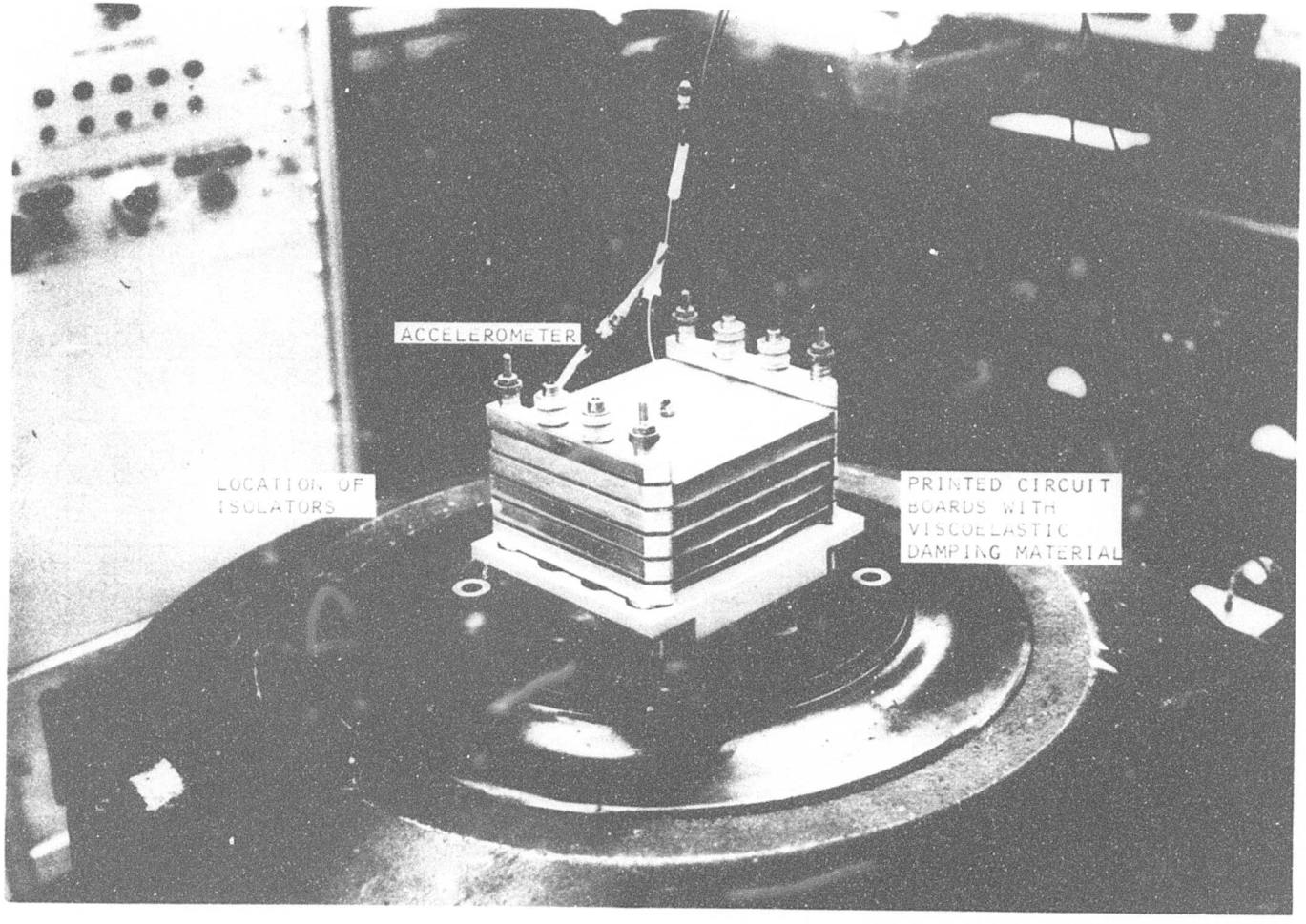

Figure 27. Vibration Test Fixture - Evaluating Damping/Isolation Concept.

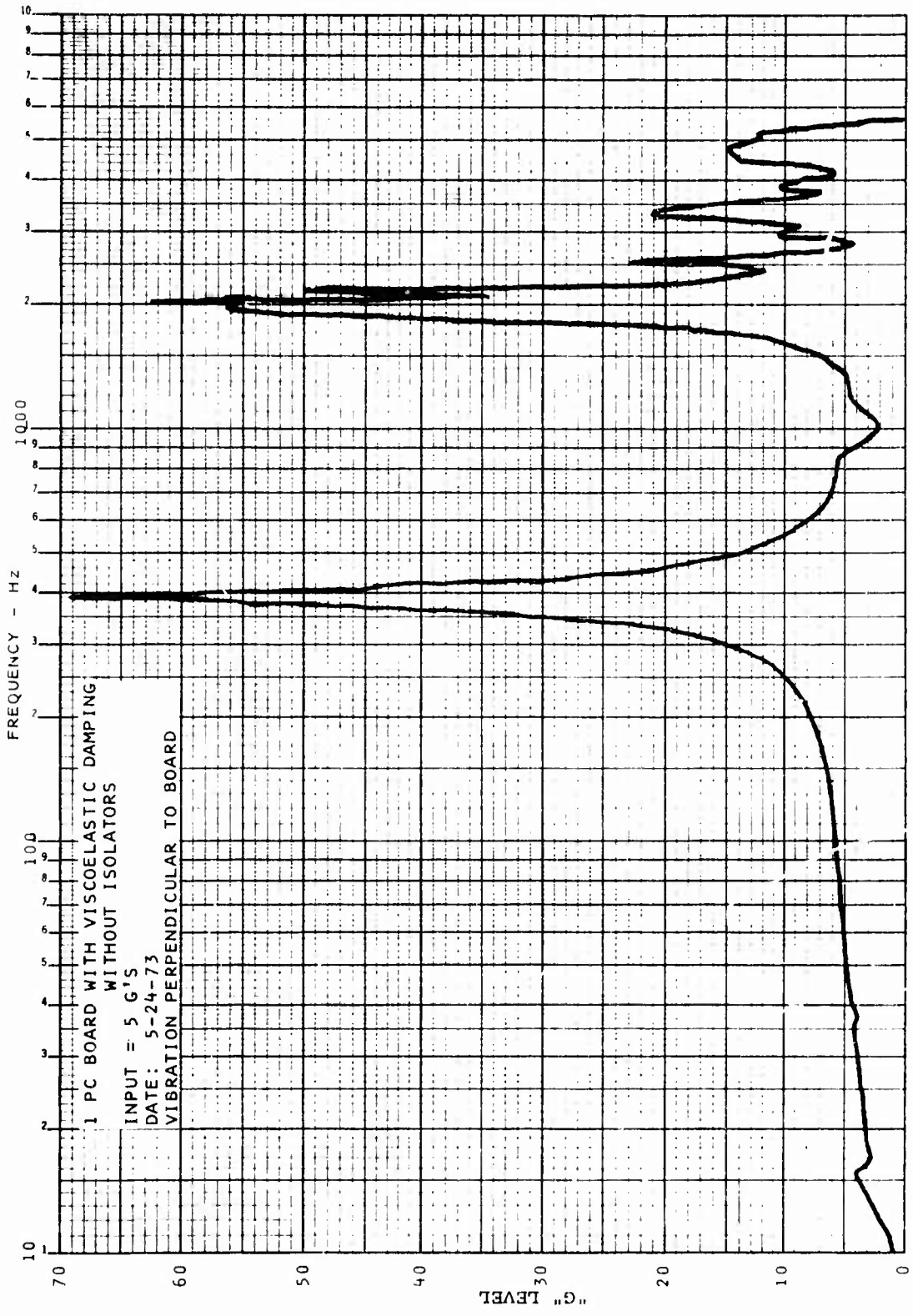

Figure 28. Printed Circuit Board Vibration Data.

closely duplicated the design value which was specified for the eight PCB design.

Figures 29, 30, and 31 show the vibration characteristics of the test assembly at 5, 10, and 20 g's input excitation in a plane perpendicular to the PCB. The results indicate that over the MIL-E-5007C frequency range, the resonant vibration of the PCB's will be limited to 30 g's. Also, the results indicate that the transmissibility decreases as the input g level increases. Consultation with the viscoelastic material manufacturer verified that this would happen. The viscoelastic material has a fiberglass backing; and when it is bonded to the PCB, a sandwich construction results. When the PCB is deflected, shear forces are generated by the viscoelastic material to provide damping. The amount of damping increases nonlinearly with the rate the board is deflected. Thereby, at the higher g levels, the damping ratio increases.

To evaluate the thermal performance of the vibration concept, the vibration test was repeated after a hot air gun had brought the assembly temperature up to 200°F. Figure 32 illustrates the results, and as predicted, an increase in temperature makes the system more "fluid", reducing the damping of the viscoelastic damping material and increasing the transmissibility of the elastomer isolator. However, the results indicate that the 30 g maximum vibration level goal is still basically met.

No attempt was made to evaluate low-temperature performance, as it was felt that the inherent stiffening of both the isolation and damping elements would provide g levels even lower than their room ambient counterparts.

To complete the vibration test evaluation, the test assembly was vibrated in a plane parallel to the PCB's. The results of this test (Figure 33) indicate only one resonant frequency which represents the fundamental frequency of the vibration isolators and five PCB test

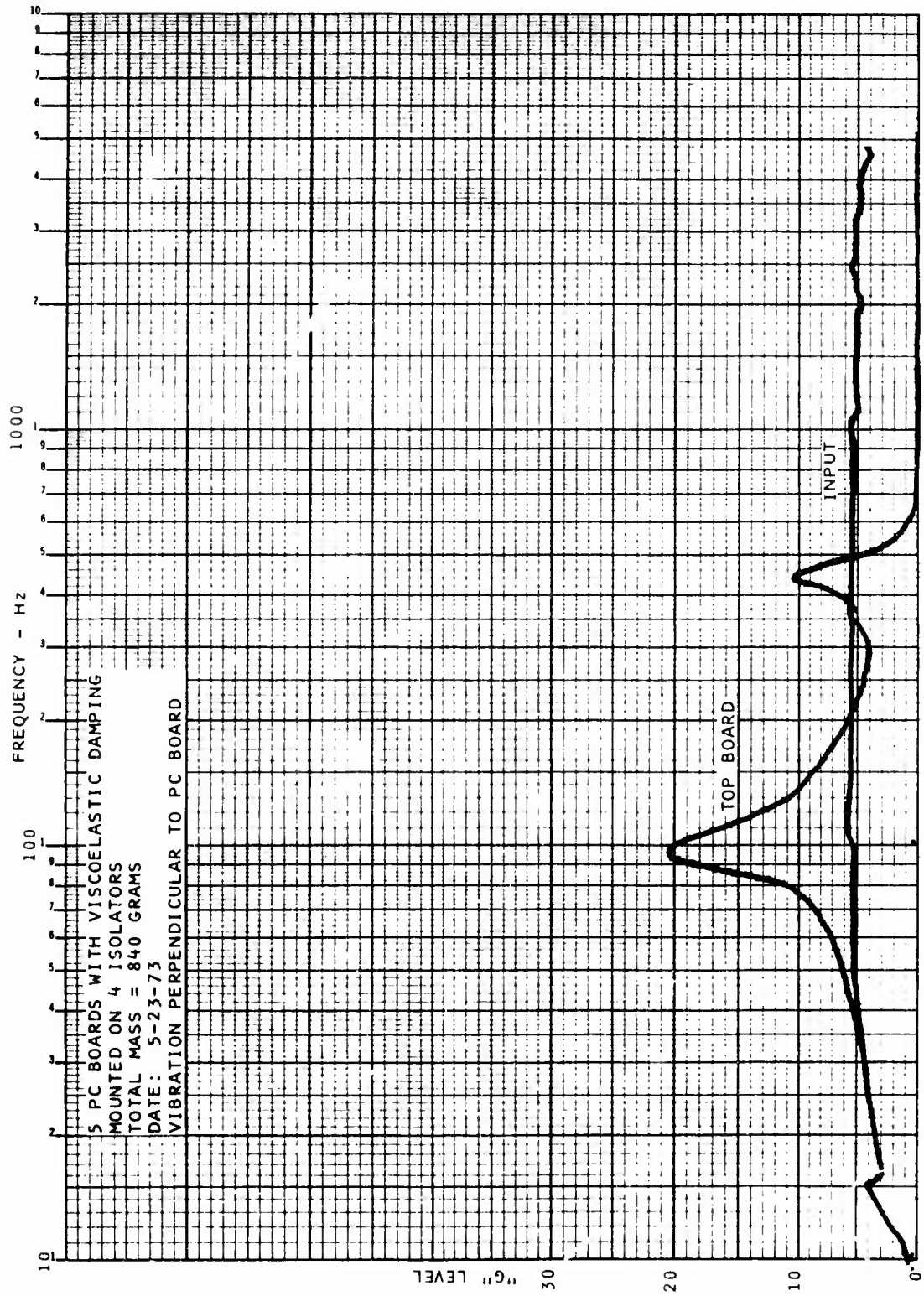

Figure 29. Printed Circuit Board Vibration Data.

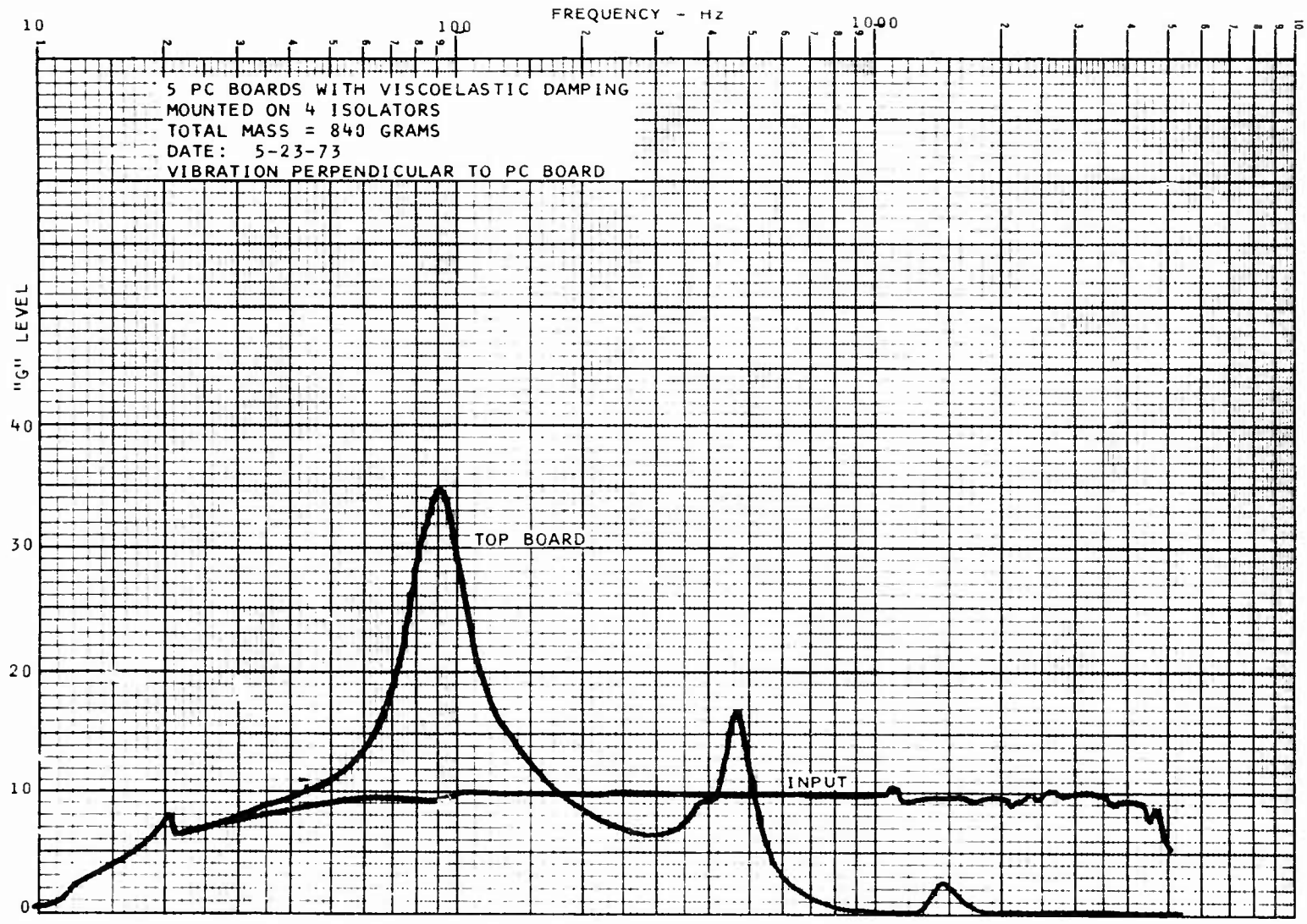

Figure 30. Printed Circuit Board Vibration Data.

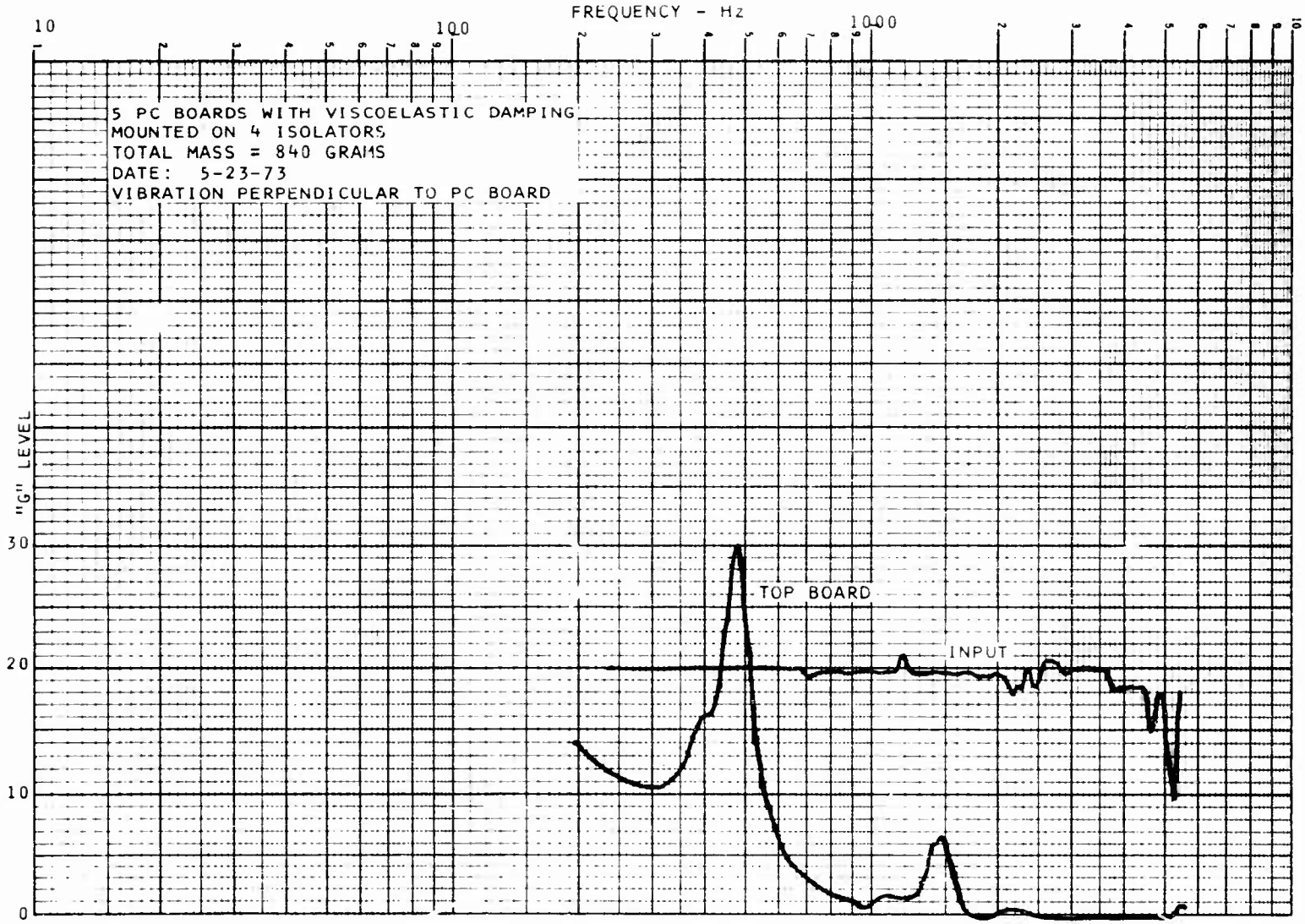

Figure 31. Printed Circuit Board Vibration Data.

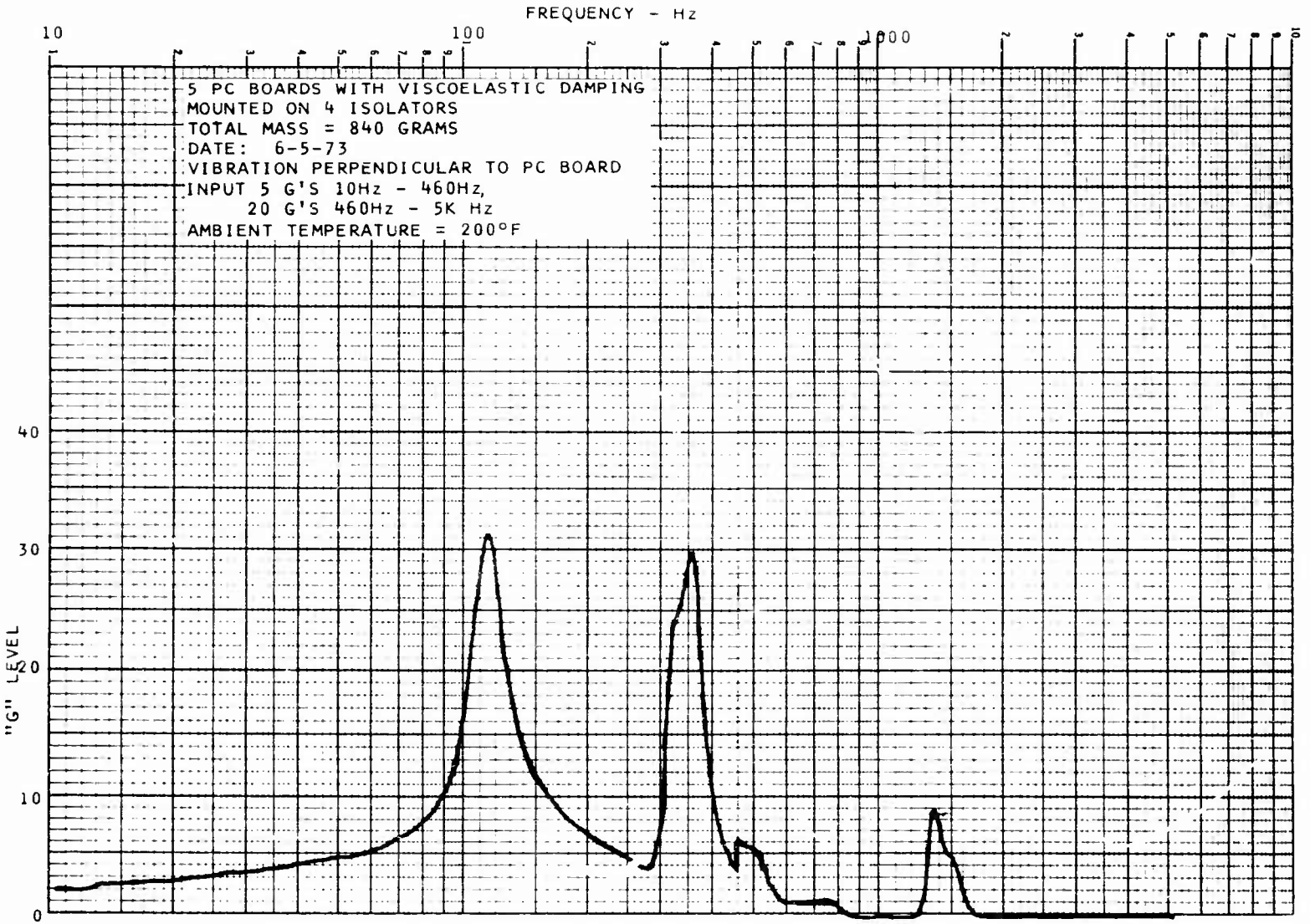

Figure 32. Printed Circuit Board Vibration Data.

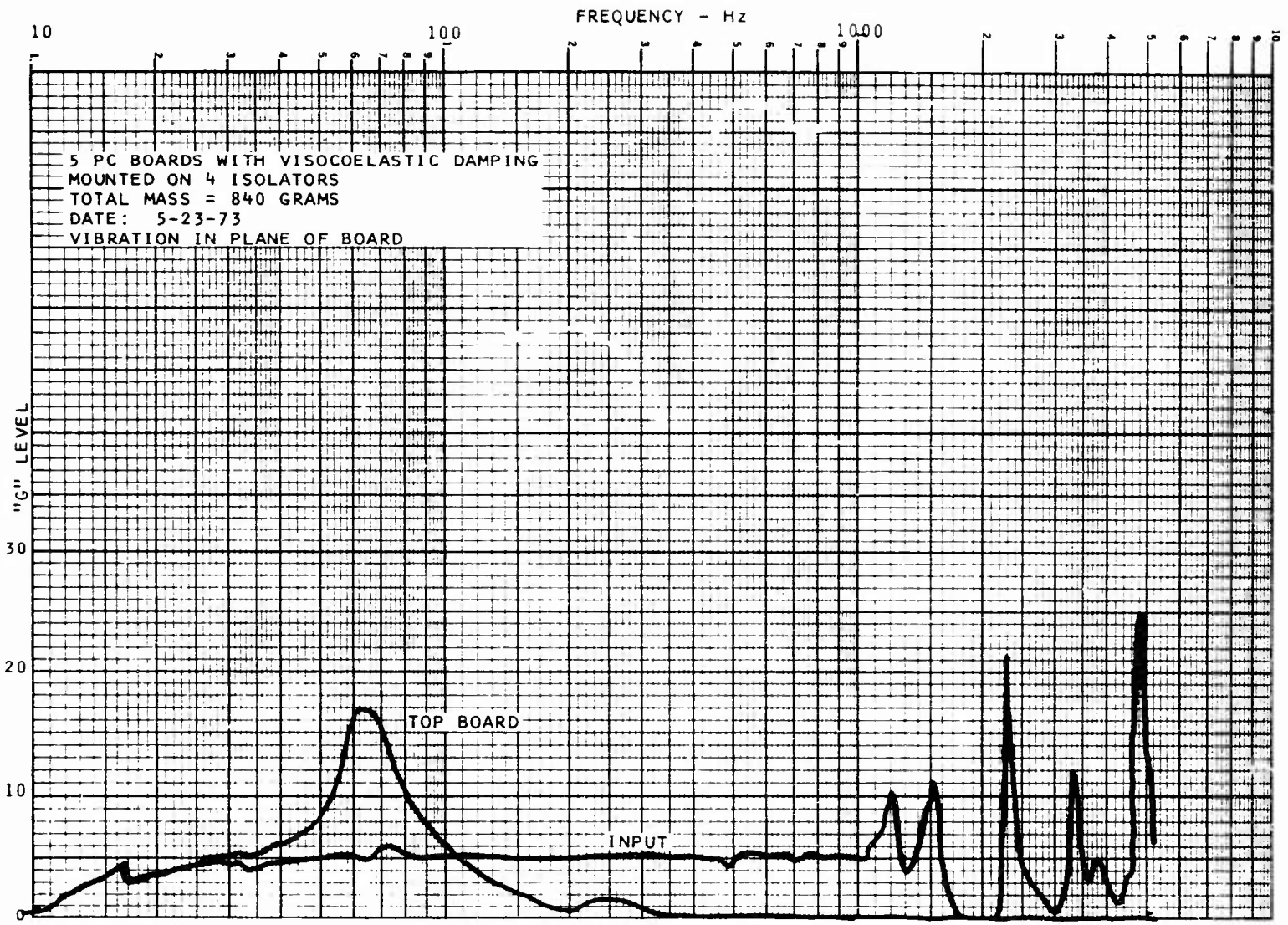

Figure 33. Printed Circuit Board Vibration Data.

assembly. The resonance associated with the input is due to the inherent limitation of the vibration table to drive the test fixture.

CONCLUSIONS AND RECOMMENDATIONS

The development work completed during this program investigated design approaches and demonstrated selected design concepts to provide solutions to the excessive centrifugal pump temperature rise problem and the thermal and vibration susceptibility of the electronic computer.

The centrifugal pump was redesigned to increase maximum speed from 37,500 to 55,000 rpm and to incorporate radial vanes instead of backward leaning vanes. The pump was demonstrated to provide acceptable fuel temperature rise over the engine operating envelope of the 5-pps-airflow engine. Test results demonstrated that by operating this pump in the vapor core mode, it would also be acceptable for operation on the 2-pps-airflow engine. Analytical studies indicate that a 75,000-rpm pump operating in the normal throttled discharge mode will provide acceptable fuel temperature rise for the 2-pps engine.

The redesigned electronic computer provides a reduction in power dissipation from the original 60 watts to approximately 7 watts. This design eliminates hot spots and self-heating problems. At 250°F ambient and 135°F fuel at the inlet to the cold plate, the hottest component case temperature was less than 200°F. The control was tested in a 180°F ambient, without any cooling, and the maximum component temperature rise was 9°F. It would therefore be possible to operate the control in an ambient temperature approaching 250°F without exceeding the 257°F maximum temperature of available electronic components. However, the design goal of limiting the maximum component temperature to 200°F will enhance reliability by reducing the temperature stress.

A variety of vibration isolation and damping concepts were evaluated. The selected scheme provides both internal vibration isolation and damping of the printed circuit boards with viscoelastic material. Vibration test results show that this system meets the design goal of limiting induced vibration to 30 g's over the specified vibration envelope. Although electronic components can be procured for operation at 50 g's, the 30 g design goal was selected to improve reliability by reducing vibration stress.

It is felt that the development work completed to date has successfully demonstrated the capability of electronic control technology for engine-mounted operation. An engine demonstration program is required to complete the evaluation of the system.

Pump performance at .45 V/L conditions was demonstrated in the original 30-month program. However, new specifications for Army aircraft engines have extended this requirement to 1.0 V/L. It is, therefore, recommended that a pump program aimed at developing a V/L = 1.0 capability with the high-speed centrifugal pump be instigated.

LITERATURE CITED

1. Daily, J. W., and Nece, R. E., FLOW PHENOMENA OF PARTIALLY ENCLOSED ROTATING DISKS, Transactions of the ASME, Vol. 82, February 1960.

2. Eckert and Drake, HEAT AND MASS TRANSFER, 2nd Ed., New York, McGraw-Hill, 1959.

3. Kays, W. M., CONVECTION HEAT AND MASS TRANSFER, New York, McGraw-Hill, 1966.

4. ELECTRONIC INTERFERENCE CHARACTERISTICS REQUIREMENTS FOR EQUIPMENT, MIL-STD-461A, 1 May 1970.

5. VIBRATION REQUIREMENTS FOR EQUIPMENT, MIL-E-5272C, 13 April 1959.

6. ENGINES, AIRCRAFT, TURBOJET AND TURBOFAN, TESTS FOR, MIL-E-5009D, 13 November 1967.

7. FLUIDS, CALIBRATION FOR AIRCRAFT FUEL SYSTEM COMPONENTS, MIL-F-7024A, 19 May 1969.

8. ENGINES, AIRCRAFT, TURBOJET, TURBOFAN, GENERAL SPEC. FOR, MIL-E-5007C, 30 December 1965.

9. JET FUEL, GRADES JP4, JP5, MIL-T-5624G-1, 30 October 1970.

10. AIRBORNE ELECTRONIC & ASSOCIATED EQUIPMENT, APPLICABLE DOCUMENTS, ANA Bulletin 400U, 5 November 1964.

11. ELECTRONIC EQUIPMENT STANDARDS, MIL-STD-454C, 15 October 1970.

12. Wills, D. F., and White, A. H., ADVANCED ENGINE CONTROL PROGRAM, Colt Industries, Inc., Chandler Evans Control System Div., USAAMRDL Technical Report 72-59, Eustis Directorate, U. S. Army Air Mobility Research and Development Laboratory, Fort Eustis, Virginia, November 1972, AD758173.

13. Chestnut and Mayer, SERVOMECHANISMS AND REGULATING SYSTEM DESIGN, 2nd Ed., Wiley 1963.

14. Harper, HANDBOOK OF ELECTRONIC PACKAGING, McGraw-Hill, 1969.

15. Keith, PRINCIPLES OF HEAT TRANSFER, International Textbook Co., 1964.

16. Manson, L. W., EXPERIENCE WITH INLET THROTTLED PUMPS, Dowty Fuel Systems, Ltd. paper presented at the joint GTD/FED Conference of the ASME, March 26-27, 1972, San Francisco, Calif. ASME Publication "GAS TURBINE PUMPS", Page 21.